PhD degree in Systems Medicine

curriculum in Human Genetics

European School of Molecular Medicine (SEMM),

University of Milan and University of Naples "Federico II"

Settore disciplinare: MED/03

IMPROVING THE THERAPEUTIC POTENTIAL OF LYSOSOMAL ENZYMES TO TREAT CNS IN LYSOSOMAL STORAGE DISORDERS

Rosanna Gilda Aiello

Tigem, Naples

Matricola n. R11742

Supervisor: Dr. Alessandro Fraldi

Tigem, Naples

Anno accademico 2019-2020

TABLE OF CONTENTS

1. ABBREVIATIONS

CLEAR coordinated lysosomal expression and regulation

TFEB transcription factor EB

bHLH basic Helix-loop-elix

NLS nuclear localization signal

mTORC1 mechanistic target of rapamycin complex 1

LYNUS lysosomal nutrient-sensing machinery

M6PR mannose-6-phosphate receptors

ER endoplasmic reticulum

CMA chaperone-mediated autophagy

LAMP2A lysosomal-associated membrane protein 2A

LSD Lysosomal Storage Disorders

MPS mucopolysaccharidosis

IDUA alpha-L-iduronidase

GAGs glycosaminoglycans

MSD multiple sulphatases deficiency

SUMF1 sulphatase-modifying factor 1

FGE formyglycine-generating enzyme

Glc-Nac UDP-N-acetyl-glucosaminyl-1-phosphotransferase

ROS reactive oxygen species

CNS central nervous system

KD Krabbe disease

PPAR-α proliferator-activated receptor-α

SNARE soluble NSF attachment proteins receptors

ML mucolipidosis

NPC Neimann-Pick

TNF-α tumor necrosis factor α

MIP-1α macrophage inflammatory protein-1α

RIPK1 Receptor Interacting Protein kinases

PD Parkinson's disease

AD Alzheimer's disease

HD Huntington disease

GOF Gain of function

α-syn α-synuclein

PSEN1 presenilin-1

Aβ β-amyloid

ERT enzyme replacement therapy

PCT pharmacological chaperones therapy

PR proteostasis regulators

HSCT hematopoietic stem cell transplantation

GT gene therapy

HSR heat-shock response

GE genome editing

ZFN zinc-finger nucleases

TALEN activator-like effector nucleases

BBB Blood-brain barrier

LV lentivirus

CRISPR/Cas9 clustered regularly interspaced short palindromic repeats/caspase 9

MLD metachromatic leukodystrophy

AAV adeno-associated virus

CSF cerebrospinal fluid

SGSH N-Sulfoglucosamine Sulfohydrolase

IDS Iduronate- 2-sulfatase

LDLR low-density lipoprotein receptor

SRT substrate replacement therapy

HB hemophilia B

GUSB β-glucuronidase

GBA β-glucosylceramidase

GLB1 β-galactosidase

h hour

rpm rotations per minute

MEF mouse embryonic fibroblast

HFF human foreskin fibroblast

GM1 gangliosidosis type 1

FBS Fetal Bovine Serum

Pen/Strep Penicillin-Streptomycin

DMEM Dulbecco's Modified Eagle Medium

Mins minutes

RT room temperature

GOF gain of function

LOF Loss of function

MOI Multiplicity of Infection

gDNA genomic DNA

Et-OH ethanol

vDNA viral DNA

4-MU 4-methylumbelliferone

2. FIGURES INDEX

3. ABSTRACT

Lysosomal storage disorders (LSD) are a large group of inherited genetic diseases caused by impaired activity of lysosomal enzymes leading to accumulation of undigested macromolecules within the lysosomes and thus cell dysfunction. The clinical manifestation is heterogeneous and neurological involvement represents a major problem.

The correction of the defective gene/protein represents the primary strategy for the treatment of these genetic conditions. However, the clinical translation of these approaches is very challenging because of the difficulty in achieving and maintaining therapeutic threshold levels of the corrective enzyme in targeted tissues (particularly in the brain) avoiding the toxicity associated to the high dosage of either viral vectors or infused corrective enzymes. To address this challenge, I have employed a strategy by which lysosomal enzymes are modified to improve their therapeutic potential. Specifically, I have developed and validated a tool through which is possible to generate gain-of-function variants of lysosomal enzymes that exhibit enhanced catalytic activity and/or increased stability in physiological conditions.

I believe that enzyme variants generated by my work may produce a beneficial effect in targeted tissues (particularly in the brain) more efficiently and therefore, at lower doses compared to the respective WT enzymes. Therefore, my data may pave the way for the development of enhanced replacement therapies with improved clinical translationability to treat CNS in multiple LSDs

4. INTRODUCTION

4.1 LYSOSOMAL STORAGE DISORDERS

Lysosomal Storage Disorders (LSD) are a large family of inherited genetic diseases, belonging to the wider group of inborn errors of metabolism (Ballabio and Gieselmann, 2009). More than 50 different types of LSDs have been described and are traditionally classified according to the chemical properties of the accumulating substrate (Table 1).

Disease	Defective protein	Main storage materials
Sphingolipidoses		
Fabry	α-Galactosidase A	Globotriasylceramide
Farber lipogranulomatosis	Ceramidase	Caramide
Gaucher	β-Glucosidase Saposin-C activator	Glucosylceramide
Globoid cell leukodystrophy (Krabbe)	Galactocerebroside β-galactosidase	Galactosylceramide
Metachromatic leukodystrophy	Arylsulphatase A Saposin-B activator	Sulphated glycolipids
Niemann-Pick A and B	Sphingomyelinase	Sphingomyelin
Sphingolipid-activator deficiency	Sphingolipid activator	Glycolipids
GM1 gangliosidosis	β-Galactosidase	GM1 ganglioside
GM2 gangliosidosis (Tay-Sachs)	β-Hexosaminidase A	GM2 ganglioside
GM2 gangliosidosis (Sandhoff)	β-Hexosaminidase A and B	GM2 ganglioside
GM2 gangliosidosis (GM2-activator deficiency)	GM2-activator protein	GM2 ganglioside
Mucopolysaccharidoses (MPS)		
MPS I (Hurler, Scheie, Hurler/Scheie)	α-Iduronidase	Dermatan and heparin sulphate
MPS II (Hunter)	Iduronate-2-sulphatase	Dermatan and heparin sulphate
MPS IIIA (San Filippo)	Heparan *N*-sulphatase (sulphamidase)	Heparan sulphate
MPS IIIB (San Filippo)	*N*-Acetyl-α-glucosaminidase	Heparan sulphate
MPS IIIC (San Filippo)	Acetyl-CoA:α-glucosamide *N*-acetyltransferase	Heparan sulphate
MPS IIID (San Filippo)	N-Acetylglucosamine-6-sulphatase	Heparan sulphate
Morquio-A disease	N-Acetylgalactosamine-6-sulphate-sulphatase	Keratan sulphate and chondroitin-6-sulphate
Morquio-B disease	β-Galactosidase	Keratin sulphate
MPS VI (Maroteaux-Lamy)	Arylsulphatase B	Dermatan sulphate
MPS VII (Sly)	β-Glucuronidase	Heparan and dermatan sulphate, chondroitin-4 and -6 sulphates

MPS IX	Hyaluronidase	Hyaronan
Oligosaccharidoses and glycoproteinosis		
Pompe (glycogen-storage-disease type II)	α-Glucosidase	Glycogen
Aspartylglucosaminuria	Aspartylglucosaminidase	Aspartylglucosamine
Fucosidosis	α-Fucosidase	Fucosides and glycolipids
α-Mannosidosis	α-Mannosidase	Mannose-containing oligosaccharides
β-Mannosidosis	β-Mannosidase	Man(β1-4)GlcNAc
Sialidosis	Sialidase	Sialyloligosaccharides and sialylglycopeptides
Schindller disease	α-N-Acetylgalactosaminidase	Glyco-conjugates
Lipidoses		
Wolman disease	Acid lipase	Cholesterol esters and triglycerides
Cholesterol-ester-storage disease	Acid lipase	Cholesterol esters and triglycerides
Diseases caused by defects in integral membrane proteins		
Cystinosis	Cystinisin	Cystine
Danon disease	LAMP2	Cytoplasmic debris and glycogen
Infantile sialic-acid-storage disease	Sialin	Sialic acid
Salla disease	Sialin	Sialic acid
Mucolipidosis (ML) IV	Mucolipin-1	Lipids and acid mucopolysaccharidea
Niemann-Pick C (NPC)	NPC1 and 2	Cholesterol and sphingolipids
Others		
Galactosialidosis	Cathepsin A	Sialyloligosaccharides
I Cells (ML II)	N-acetylglucosaminyl-1-phosphotransferase	Oligosaccharides. mucopolysaccharides and lipids
pseudo-Hurler polydystrophy (ML III)	N-acetylglucosaminyl-1-phosphotransferase	Oligosaccharides. mucopolysaccharides and lipids
Multiple sulphatase deficiency	Cα-formyglycine-genetaring enzyme	Sulphatides
Neuronal ceroid lipofuscinosis (NCL I/ Batten disease)	CLN1 (protein palmitoylthioesterase-1)	Lipidated thioesters
NCL II (Batten disease)	CLN2 (tripeptidyl amino peptidase-1)	Subunit C of the mitochondrial ATP synthase
NCL III (Batten disease)	Arinine transporter	Subunit C of the mitochondrial ATP synthase
Pycnodysostosis	Cathepsin K	Bone proteins including collagen fibrils

(Futerman and Van Meer, 2004)

Table 1. Lysosomal storage disorders, relative defective proteins and storage materials.

Although defined as rare disorders, when taken singularly, LSDs have a combined incidence estimated around 1:5000 live births (Fuller, Meikle and Hopwood, 2006), not mentioning the undiagnosed or misdiagnosed cases (Platt, Boland and van der Spoel, 2012). The majority of LSDs are caused by impaired activity of lysosomal hydrolytic enzymes leading to accumulation of undigested macromolecules within the endosomal–autophagic–lysosomal system and thus cell dysfunction (Futerman and Van Meer, 2004). However, the accumulation of monomeric catabolic products resulting from efflux deficiency greatly perturbs cellular homeostasis as well (Platt, Boland and van der Spoel, 2012). When macromolecules and monomers accumulate at high amounts in endo-autolysosomes, consequently, even the activity of catabolic enzymes and permeases not genetically mutated is impaired leading to secondary substrates accumulation (Prinetti *et al.*, 2011). Unfortunately, the lack of knowledge about the downstream biochemical and cellular pathways triggered by abnormal storage of material only gives us a partial view on such a heterogeneous group of diseases (Futerman and Van Meer, 2004). Both non-enzymatic soluble lysosomal proteins and integral membrane protein have shown to be causative of a considerable number of diseases (Saftig and Klumperman, 2009). In fact, the delivery of a defective lysosomal enzyme is only responsible for a part of lysosomal disorders, among these, we found the Mucopolysaccharidosis Type I (MPSI) or alpha-L-iduronidase (IDUA) deficiency. The IDUA enzyme is a hydrolase which breaks down a molecule known as unsulfated alpha-L-iduronic acid, which is present in two glycosaminoglycans (GAGs) called heparan sulfate and dermatan sulfate. The result of IDUA dysfunction is the accumulation of GAGs within the lysosomes.

Defective regulatory proteins required for optimal hydrolases' activity can as well cause LSDs. Therefore, one defective gene can be responsible for the dysfunction of several other proteins (Hopwood and Ballabio, 2001). An example is multiple

sulphatases deficiency (MSD) a very rare condition resulting from mutations (12 identified so far) of the sulphatase-modifying factor-1 gene (SUMF1) encoding for the Cα-formyglycine-generating enzyme (FGE). When this enzyme is missing, a specific cysteine residue common to all the 13 known suplhatases cannot be converted into a Cα-formyglycine resulting in the reduced activity of all the members of the family. Alternatively, a defective glycosylation could result in an enzyme with reduced catalytic activity or a dysfunction in the mannose-6-phosphate pathway can impair enzyme entrance into the organelles. This is the case of two mucolipidosis, the Inclusion-cell (I-cell) disease (mucolipidosis II - MLII) and the Pseudo-Hurler polydystrophy (mucolipidosis III - MLIII), which result from a defective phosphotransferase: the UDP-*N*-acetyl-glucosaminyl-1-phosphotransferase (Glc-Nac) (Kornfeld and Sly, 2001). This enzyme phosphorylates mannose residues to mannose-6-phosphate in the Golgi. Without mannose-6-phosphate to target them to the lysosomes, the enzymes are erroneously secreted by the cell (Dittmer *et al.*, 1999). Eventually, integral membrane proteins like ions transporters and other proteins involved in the maintenance of lysosome homeostasis may be at the basis of a pathological mechanism. A main example is represented by the sialic-acid-storage disorders (SASD), where a defective ion transporter (Sialine) is not able to export soluble metabolites out of the lysosomes (Mancini, Havelaar and Verheijen, 2000). Another example is Danon disease, where mutations in LAMP2, specifically in its highly glycosylated transmembrane domain, lead to the accumulation of vacuoles containing cytoplasmic debris in muscles (Nishino *et al.*, 2000).

The intracellular storage accumulation affects not only the endo-auto-lysosomal system but also impacts on other cellular components such as the endoplasmic reticulum (ER) and the Golgi, the nucleus, mitochondria, peroxisomes and plasma membrane thus altering the overall cellular function (Platt, Boland and van der

Spoel, 2012). The ER is mainly affected in its function of calcium homeostasis regulator. In sphingolipid storage disorders the accumulating lipids affect ER calcium channels function leading to increased cytosolic calcium levels. While ER stress and thus unfolded protein response has been only described in GM1 gangliosidosis so far (Tessitore *et al.*, 2004; Vitner, Platt and Futerman, 2010). Golgi dysfunction is also common in lipid storage disorders where usually the sphingolipids trafficking is impaired. However, in mucopolisaccaridosis Type IIIB (San filippo B syndrome) Golgi matrix protein (GM130) enriched storage bodies reveal an impaired capacity of vesicles formation; in addition, an altered Golgi morphology accompanied by LAMP1-positive storage bodies suggests that probably Golgi biogenesis is affected as well (Vitry *et al.*, 2010). Reduced autophagy particularly affects mitochondrial function as dysfunctional mitochondria, which are normally constitutively degraded (mitophagy), are instead retained in the cytoplasm where they accumulate and generate reactive oxygen species (ROS) that make cells more susceptible to apoptotic and inflammatory stimuli (Kim, Rodriguez-Enriquez and Lemasters, 2007; Terman *et al.*, 2010). Maybe, aberrant mitochondrial function is for this reason responsible for inflammation processes involved in central nervous system (CNS) pathology of multiple LSDs (Platt, Boland and van der Spoel, 2012). Peroxisomal dysfunction also occurs in some lipid lysosomal disorders. In particular in Krabbe disease (KD) accumulating galactosylsphingosine down-regulates the peroxisome proliferator-activated receptor-α (PPAR-α) which promotes the uptake and catabolism of fatty acids by the upregulation of genes involved in fatty acid transport, binding and activation, and peroxisomal and mitochondrial fatty acid β-oxidation (Haq *et al.*, 2006). Moreover, gangliosides specifically accumulating in peroxisomal biogenesis disorders are also often found as secondary storage metabolites in many LSDs

suggesting that peroxisomes may play a role in secondary ganglioside storage in LSDs (Platt, Boland and van der Spoel, 2012).

4.1.1 CLINICAL FEATURES

LSDs are mainly monogenic, and in most cases, multiple mutations have been identified for each gene. Interestingly, for some diseases, patients carrying the same mutation may display a very different spectrum of symptoms from severe to almost asymptomatic. For this reason, for most of them, an obvious correlation genotype-phenotype has not been described and no prediction, starting from a given genetic condition, can be made about the progression of the disease (Futerman and Van Meer, 2004).

The clinical manifestation is heterogeneous as both systemic and neurological symptoms may occur at different ages and progress at different rates among patients (Fraldi *et al.*, 2016). Child affected by LSDs generally do not present any sign of the disease at the time of birth as symptoms develop during the first year of life (Ferreira and Gahl, 2017); only in rare cases fetuses can exhibit pathological signs (Adachi, Schneck and Volk, 1974). LSDs exist in severe infantile forms, intermediate juvenile, and mild adult forms. Infantile LSDs usually present severe brain involvement and lead to the death of the patient within the first decade of life. As the pathology progresses children can experience vision disturbances (among the first symptoms), seizures, hearing loss, dementia, brain stem dysfunction and neuromotor regression (Futerman and Van Meer, 2004; Fraldi *et al.*, 2016). In juvenile and adult forms, symptoms arise more slowly and may include depression, dementia and psychosis, and in some cases (late adult onset) mainly remain peripheral including hepatosplenomegaly, heart and kidney damage, impaired osteogenesis and muscular atrophy (Futerman and Van Meer, 2004). Anyway, each LSD has a peculiar clinical and pathological picture that depends on

the degree of protein function affected, on the biochemistry of the accumulated material and on the cell types affected by the storage alteration (Platt, Boland and van der Spoel, 2012). Most LSDs exhibits CNS involvement with neurodegeneration following a temporal and spatial specific pattern. Before global brain degeneration occurs, certain regions seem to be preferentially interested by neurodegeneration and inflammation. This probably happens because each neuronal population synthetizes specific macromolecules and responds to different stored metabolites in specific ways (Platt, Boland and van der Spoel, 2012). The activation of the immune system also plays a fundamental role in processes leading to CNS pathology in LSDs. In particular, astrocytes activation (astrogliosis) is common in lysosomal diseases and induces neuronal loss through an inflammatory process called glial scarring (Vitner, Platt and Futerman, 2010). However, immunological alterations are also characteristic of some LSDs where no CNS involvement in present. In Type 1 Gaucher disease, for example, glucosylceramide accumulates in macrophages more than in any other cell type resulting in impaired capacity of hematopoietic cells production and turnover and in macrophages infiltrating into organs and affecting their functions (Platt, Boland and van der Spoel, 2012). In particular, the neurological involvement represents a major problem as it may manifest with severe symptoms, and is present in nearly two-third of the patients affected by LSDs (Passarge, 2001; Saftig and Klumperman, 2009).

4.1.2 PATHOGENIC MECHANISMS

Lysosomal function

Lysosomes are membrane-bound cytoplasmic organelles with a diameter from 0.05μm to 0.5μm, generating an acidic environment (pH=4,5-5) where a variety of hydrolases and other proteins synergistically work to break up both intracellular

and extracellular macromolecules into their terminal components (Passarge, 2001).

Both lysosomal enzymes and extracellular macromolecules can enter the lysosome by receptor-mediated endocytosis (Passarge, 2001). Specifically, nascent hydrolases among which we find sulfatases, phosphatases, glycosidases proteases, lipases and nucleases bind to mannose-6-phosphate receptors (M6PRs) in the trans-Golgi, which transports them to early and then to late endosomes (Ghosh, Dahms and Kornfeld, 2003). The fusion of late endosomes with lysosomes eventually delivers the digestive enzymes into the lysosomal compartment (Platt, Boland and van der Spoel, 2012). Extracellular macromolecules bind to specific receptors on the cell surface that, once loaded, concentrate to generate an invagination of the plasma membrane called “coated pit”. From the invagination originates a coated vesicle, a membrane-bound cytoplasmic element that moves from the limiting membrane. Early endosomes form when the vesicles lose their clathrin coat. At this stage, they have the capability to fuse with other membrane vesicles coming from the Golgi to become larger (late) endosome that eventually fuse with lysosomes (Passarge, 2001). Intracellular material is transported to the lysosomes through autophagic pathways (Saftig and Klumperman, 2009). Autophagy induces the lysosomal degradation of intracellular cytosolic component in order to maintain cellular energy and homeostatis (Settembre *et al.*, 2013). Three different types of autophagy have been described, all three culminating in lysosomal degradation: macroautophagy, microautophagy and chaperone-mediated autophagy (Mizushima, 2007). Macroautophagy is the most common form of autophagy (Mizushima, 2007); it relies on the formation of membrane-enclosed vesicles (AVs or autophagosomes) that generate at the contact sites between the ER and mitochondria (Hamasaki *et al.*, 2013). The macromolecules such as lipids, carbohydrates, RNA and

organelles are sequestered by AVs through a receptor-mediated system (Eskelinen and Saftig, 2009; Rogov *et al.*, 2014), trafficked to the lysosomes and delivered upon fusion of AVs with lysosomes. In microautophagy lysosomes confiscate cytosolic portions through the invagination of their membranes (pinocytosis). Whereas, in chaperone-mediated autophagy (CMA) proteins containing a pentapeptide (KFERQ) degradation motif enter lysosomes through direct protein-protein interaction. Specifically, the heat shock protein of 70 kDa (Hsc70) binds proteins to be degraded docking them on lysosomes through contact with lysosomal-associated membrane protein 2A (LAMP2A) and their subsequent entering into the lysosomes (Eskelinen, 2006). Macromolecules are here disassembled to recover their elementary components (monosaccharides, amino acids and fatty acids) that exit the lysosome to be re-employed either for the biosynthesis of new molecules or as a source of energy (Passarge, 2001; Fraldi *et al.*, 2016). Since the acidic pH within the lysosomes is necessary for the optimal functioning of lysosomal enzymes, proteins like ion channels and transporters responsible for its maintenance are crucial to the entire lysosomal system like the proton-pumping V-type adenosine triphosphatase (ATPase) (Mindell, 2012). Several proteins involved in inward lysosomal trafficking have been characterized like potassium and calcium channels (Cang *et al.*, 2015) and chloride channels (Graves *et al.*, 2008); little is known, instead, about the lysosomal efflux system. A very exiguous number of transporters have been identified involved in the efflux of amino acids, sugars and cholesterol (Fraldi *et al.*, 2016).

Since their discovery by Christian De Duve in 1995, up to recent times, lysosomes were believed to be static organelles only responsible for waste material clearance (Napolitano and Ballabio, 2016). On the contrary, lysosomal biogenesis and function are transcriptionally finely regulated processes (Sardiello *et al.*, 2009). A gene network known as the coordinated lysosomal expression and regulation

(CLEAR) network regulates lysosomal biogenesis (Sardiello *et al.*, 2009; Palmieri *et al.*, 2011). The expression of these lysosomal genes is differentially regulated in different cell type and according to cellular requirements (Sardiello *et al.*, 2009). The CLEAR sequence is the binding site for the master regulator of the entire lysosomal genes network: transcription factor EB (TFEB) (Sardiello *et al.*, 2009; Palmieri *et al.*, 2011). It directly controls the expression of lysosomal genes; it activates them and enhances their expression and thus lysosomes formation and substrate degradation. Moreover, its role in the regulation of autophagy genes and lysosomal exocytosis has been demonstrated (Sardiello *et al.*, 2009; Palmieri *et al.*, 2011). Specifically, it induces autophagosomes biogenesis and their fusion with lysosomes (Ballabio *et al.*, 2011), and lysosome fusion with the plasma membrane and the subsequent secretion of their content into the extracellular compartment (Medina *et al.*, 2011). TFEB regulation is modulated by post-translational modifications (Martina *et al.*, 2012; Roczniak-Ferguson *et al.*, 2012). Among the multiple kinases that phosphorylate TFEB the mechanistic target of rapamycin complex 1 (mTORC1) is considered its main regulator. mTORC1 is a serine/threonine kinase involved in cell growth and cellular metabolism maintenance (Laplante and Sabatini, 2012). In nutrient-rich conditions, mTORC1 inhibits TFEB activation (Ballabio *et al.*, 2011; Martina *et al.*, 2012; Roczniak-Ferguson *et al.*, 2012). mTORC activation itself is regulated by the lysosome and upon starvation it is indeed released from the lysosomal membrane into the cytoplasm where it becomes inactive (Sancak *et al.*, 2010). In addition, MTORC1 can also induce new lysosomes formation through autophagic-induced reactivation when, during growth factors-induced autophagy, autolysosome formation and lysosomal consumption increase (Yu *et al.*, 2010).

The dysfunction of a single element of such a complex system is sufficient to induce the accumulation of undigested macromolecular substrates within the

lysosomal compartment with subsequent detrimental effects on cellular homeostasis (Passarge, 2001).

CNS pathology in LSDs

The neurological defects characteristic of many LSDs are associated with morphological changes in neuronal structure caused by neurodegeneration and inflammation processes affecting different neuronal populations in a peculiar way for each LSD (Ghosh, Dahms and Kornfeld, 2003; Saftig and Klumperman, 2009). Up to date, the pathogenic processes contributing to neurodegeneration in LSDs are still unclear. One hypothesis relies on impaired autophagy as the mediator of neurodegeneration (Settembre *et al.*, 2008). Neurons of some mouse models of lysosomal disorders show the accumulation of polyubiquitinilated proteins and dysfunctional mitochondria resembling what happens in neurodegeneration experiments where genetically inhibited autophagy leads to ultimate neuronal death (Hara *et al.*, 2006). Lysosomes filled with undigested materials fail to fuse with autophagosomes as a result the cytoplasm fills up with undigested autophagosomes, mitochondria and aggregates positive for the autophagy receptor P62 (de Pablo-Latorre *et al.*, 2012; Lieberman *et al.*, 2012). This is probably due to impaired lysosomal reformation with the subsequent block of AVs-lysosomes fusion since cells derived from patients affected by different LSDs showed impaired mTORC reactivation (Yu *et al.*, 2010). In addition, the secondary accumulation of cholesterol in endosomal membranes affects the soluble NSF attachment proteins receptors (SNAREs) function, which are fundamental components of the membranes fusion machinery (Fraldi *et al.*, 2010). Moreover, the intracellular accumulation of lipids affects lysosomal calcium homeostasis, which also contributes to regulating lysosomal trafficking. Specifically, mutations in the lysosome calcium channel TRPML1 have been proposed as responsible for

the perturbation of calcium homeostasis in some LSDs as well as to be the primary cause of mucolipidosis type IV (ML-IV) (Vergarajauregui and Puertollano, 2008; Medina *et al.*, 2015). While, in Neimann-Pick disease type C1 (NPC1) sphingomyelin accumulates inhibiting TRPML1 activity, and, since sphingomyelis accumulate in a variety of LSDs, TRPML1 dysfunction may in fact play a crucial part in their pathogenesis (Shen *et al.*, 2012).

A second hypothesis for neurodegeneration in lysosomal diseases relies on a non-cell autonomous mechanism where neuronal death occurs because of the altered activity of CNS-resident cells responsible for neurons support and maintenance of brain homeostasis. For example, astrocytes perform many functions in the CNS, including the provision of nutrients to the nervous tissue, trafficking and recycling of neurotransmitters, maintenance of extracellular ions balance and protection against oxidative stress. Their role in the neuropathology of LSDs has been evidenced both in vitro and in vivo. Experiment on MSD mice revealed cortical neurons degeneration when the lysosomal storage disorder was selectively induced in astrocytes alone (Di Malta *et al.*, 2012). Consistently, astrocytes dysfunction is also been associated to behavioral alterations related to cortical neurons loss. Cultured astrocytes from LSDs revealed an impaired capacity of retaining glutamate that induces neuronal excitotoxicity when released in the extracellular space (Di Malta *et al.*, 2012; Sáez *et al.*, 2013). In addition, astrocytes seem to be very sensitive to the lipid droplets characteristic of some LSDs. Lysosomes regulate lipid droplets homeostasis thus when lysosomal function is impaired the resulting accumulated lipids build up in lipids droplet and astrocytes result stressed enough to trigger neuronal degeneration (Singh *et al.*, 2009; Liu *et al.*, 2015). Microglial activation is also characteristic of LSDs. Microglial cells are CNS-resident immune cells that play the same role macrophages play in non-neuronal tissues. In many LSDs interested by neurodegeneration the microglial

population activates and expands probably in the attempt to remove damaged neurons. In fact, microglial cells show a massive vacuolization and storage probably due not only to endogenous accumulation because of the genetic condition but also to the phagocytic activity. This happens in a general inflammatory state characterized by increased levels of inflammation mediators such as cytokines (interleukins, tumor necrosis factor-α (TNF-α), macrophage inflammatory protein-1α (MIP1α)) and ROS that further worsens neurons condition (Wu and Proia, 2004; Di Malta *et al.*, 2012; Vitner, Futerman and Platt, 2015). Notably, microglial activation has been found to be associated with neuronal death processes specifically when it is driven by necroptosis or necrosis, normally employed by neurons when autophagy is impaired. Suggesting that the inflammatory response may as well ultimately result from defective autophagy (Enquist *et al.*, 2007). As an evidence, necroptosis and the consequent neuroinflammation are prominent in Gaucher's disease neurons due to caspase-8 dysfunction leading to the activation of two members of the Receptor Interacting Protein (RIP) kinases family (RIPK 1 and 3) which transduce inflammatory and cell death signals triggered by the activation of death receptors (Vitner, Futerman and Platt, 2015).

Lysosomal dysfunction has also been described in other neurodegenerative diseases such as Parkinson's disease (PD), Alzheimer's disease (AD) and Huntington disease (HD). The study of these diseases gave a consistent help in further understanding the link between lysosomal dysfunction and neuronal loss (Nixon, Yang and Lee, 2008; Fraldi *et al.*, 2016). Seen the late onset of these pathologies, aging processes have been also investigated to understand whether age-related changes may affect intracellular protein degradation. In fact, both lysosomal hydrolases and lysosomal membrane components revealed to be affected by age-related modifications. As an example, LAMP-2a levels reduces

with time in both liver cells of old rats and late-passage human fibroblasts, resulting in impaired substrate binding to lysosomes and thus in decreased chaperone-mediated autophagy (Cuervo and Dice, 2000).

The peculiar aggregations composed of gain-of-function (GOF) protein variants that characterize the cited neurodegenerative disorders provided new insight in the pathogenic processes originating from lysosomal dysfunction (Fraldi *et al.*, 2016). PD is one of the most common neurodegenerative disorders and is characterized by intracellular deposits of α-synuclein (α-syn) known as Lewy bodies. A-Syn is an aggregate-prone protein common to a group of neurodegenerative diseases called synucleopathies (Spillantini *et al.*, 1997). The mutant aggregated protein is able to bind to lysosomal membrane receptors and disrupt its own degradation pathway, and that of other substrates, carried out by chaperone-mediated autophagy, by blocking molecules uptake from the receptors (Cuervo *et al.*, 2004).

Instead, wild type α-syn deposits impair macroautophagy through inhibition of Ras-related protein Rab-1A (Rab1a) (Winslow *et al.*, 2010) and their endocytosis can induce the rupture of lysosomes leading to increase in ROS (Freeman *et al.*, 2013). In neuronal cells, aggregated α-syn is able to retain TFEB in the cytoplasm as it shares structural similarity with 14-3-3 proteins and is able to bind similar targets (Cuervo *et al.*, 2004). Interestingly, α-synuclein has been found to accumulate in some LSDs (Shachar *et al.*, 2011), at the same time, mutations in lysosomal genes have also been associated with an increased risk of developing PD. A case in point is GBA deficiency. Heterozygous mutation of GBA lead to increased intracellular levels of glycosilceramide that can stabilize soluble α-syn precursors that are converted in amyloid fibrils. In addition, the accumulating α-synuclein itself blocks GBA shuttling to the lysosomes further increasing glucosylceramide accumulation (Mazzulli *et al.*, 2011). Moreover, the study of the mouse model of MPS IIIA demonstrated that multiple amyloid proteins including α-

synuclein, prion protein (PrP), Tau, and amyloid-β progressively aggregate in the brain. The buildup of amyloid deposits with a gain-of-function mechanism in neuronal cell bodies, correlate with neurodegeneration (Monaco *et al.*, 2020). In addition, α-syn also acts as key chaperon responsible for the proper functioning of synaptic SNAREs and thus synaptic vesicle recycling and presynaptic terminal transmission (Burré *et al.*, 2010). Its accumulation as neuronal insoluble aggregates and showed that this accumulation depletes synaptic a-synuclein, contributing to neurodegeneration by a loss-of-function mechanism (Sambri *et al.*, 2017). Therefore, its accumulation and dysfunction may also contribute to neurodegenerative processes by inducing presynaptic failure in LSDs (Fraldi *et al.*, 2016).

AD patients show lysosomal dysfunction because of alteration in the lysosomal acidification machinery and Ca+ homeostasis in some cases related to the mutation of the presenilin-1 (*PSEN1*) gene (Lee *et al.*, 2010, 2015). The pathologic accumulation of β-amyloid (Aβ) peptides is indeed caused by impaired endolysosomal recycling trafficking, which is responsible for the processing of amyloids precursors into mature proteins (amyloidogenic process) (Rajendran and Annaert, 2012). Eventually, in HD an abnormal huntingtin protein with polyglutamine expansions probably affects autophagy as it results poorly recognized by autophagosomes (Walker, 2007; Jeong *et al.*, 2009).

4.2 THERAPIES FOR LSDs: State of the art

Up to date the treatment of LDSs is very challenging because of the enormous variability that characterizes these disorders from their genetic causes, passing through the pathogenic mechanisms involved, to their clinical aspects. Although, during the past 20 years, remarkable progresses have been made particularly with the development of innovative therapeutic strategies (Parenti *et al.*, 2013).

Each step of the pathogenic cascade leading to primary and secondary substrates accumulation and cell dysfunction represents a possible target for the therapy. The primary purpose of treatments is to provide cells with the missing enzymatic activity responsible for the accumulation of material. The great majority of the established therapeutics strategy to treat LSDs is aimed at increasing the missing enzyme function by restoring its activity or replacing the dysfunctional enzyme. Such strategies include enzyme replacement therapy (ERT), hematopoietic stem cell transplantation (HSCT), small molecules pharmacological chaperones (PCT), proteostasis regulator (PR), and gene therapy (GT) and their combinations. When neither restoring nor replacing the activity of a dysfunctional enzyme/protein is possible, an alternative strategy may be reducing the synthesis of the stored substrates (Parenti *et al.*, 2013) (Figure 1, adapted from Favret *et al.*, 2020).

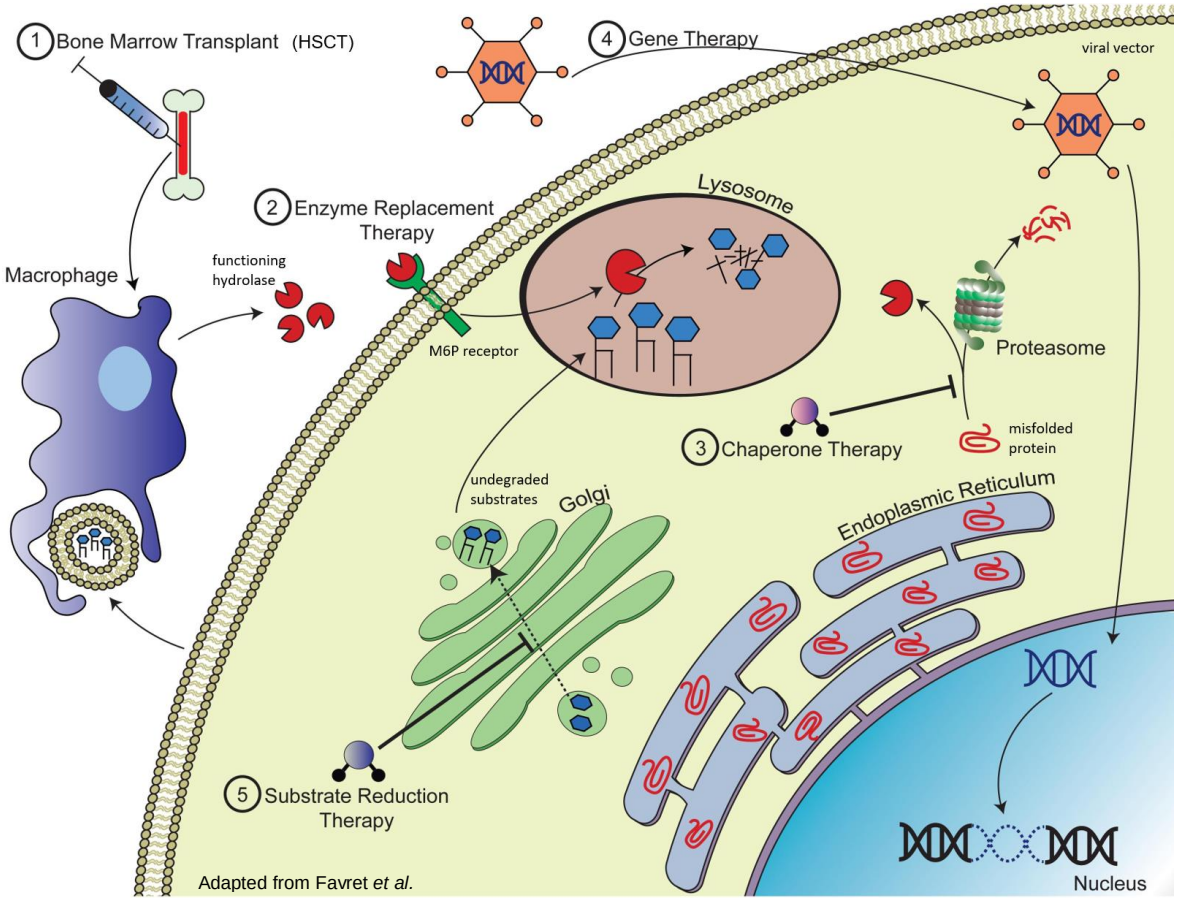

Figure 1. Therapeutic approaches for lysosomal storage disorders. (1) Bone marrow transplantation for the delivery of hematopoietic cell progenitors able of cross-correction through the production of functioning hydrolases. (2) Enzyme replacement therapy for the replacement of endogenous impaired lysosomal hydrolases with functioning recombinant hydrolases. (3) Pharmacological chaperone therapy for the restoration of correct folding of misfolded inactive endogenous lysosomal proteins. (4) Gene therapy for the delivery of recombinant DNA for the production of functioning lysosomal proteins. (5) Substrate reduction therapy for the reduction of specific accumulating substrate biosynthesis.

4.2.1 ENZYME REPLACEMENT THERAPY

Enzyme replacement therapy (ERT) has been the very first effective treatment for LSDs and today it still represents the most successful approach. It is based on the replacement of a dysfunctional enzyme with its functioning wild-type version. It consists in the periodical systemic administration of a wild type enzyme produced with recombinant DNA techniques. The infused enzyme is taken up by cells through the M6PRs expressed at the plasma membrane and is internalized and trafficked to the lysosomes through the canonical endocytic route. Once inside the

lysosomal compartment it compensates the dysfunctional endogenous enzyme. The first available ERT treatment was developed in 1990 to treat Gaucher's disease (Barton *et al.*, 1991). Since then, ERT treatments have become available for many disorders including Fabry disease, Pompe disease, mucopolysaccharidoses (I, II, IIIA, IV, VI and VII), metacromatic leukodistrophy and acid lipase deficiency. ERT demonstrated to be effective in reducing substrate accumulation, organs alterations and, in some cases, improving their function. Despite its success, however, ERT shows main limitations related to the bioavailability of recombinant enzymes. Because of their large size, recombinant enzymes are not able to freely diffuse across membranes and thus are unable to reach therapeutic levels in some organs. As a result, some patients only show limited clinical amelioration, like in MPSI where both bones and heart are mainly affected but remain refractory to the treatment. More important is the inability of enzymes to cross the Blood-brain barrier (BBB) and reach the CNS (S. Anson, McIntyre and Byers, 2011). The BBB creates an independent compartment that separates the CNS from the rest of the body. It has a neuroprotective role as it creates a very stable ionic environment necessary for synaptic transmission and prevents the exposition of the CNS to both endogenous and exogenous neurotoxic molecules (Begley, Pontikis and Scarpa, 2008). It also excludes exogenous lysosomal enzymes from the brain representing a major problem as nearly two thirds of LSDs show main CNS involvement with severe and progressive neurodegeneration. Two phase I/II studies (Jones *et al.*, 2016; Giugliani *et al.*, 2017) demonstrated that it is possible to achieve amelioration of CNS manifestation through ERT respectively in MPSIIIA and MPSI. In the former, the delivery of the wild type enzyme directly into the CNS was performed through intrathecal infusion and lead to a significant decline in GAGs levels (Jones *et al.*, 2016). In the latter, a chimeric version of IDUA fused with a monoclonal antibody

against the human insulin receptor administrated intravenously showed to be able to cross the BBB and improve neurological functions in patients (Giugliani *et al.*, 2017). The efficacy and reliability of these approaches need further confirmation.

It is important to underline that to achieve clinical efficacy it is imperative to initiate ERT treatments at early stages of the disease as irreversible organ damages may not respond if treated too late (Beck, 2018). The elevated costs of ERT treatments also represent a significant limitation to its employment in public health. In particular, the production of a recombinant enzyme requires conspicuous annual investments for a single patient needing life-long treatments thus limiting the access of patients to ERT (Parenti *et al.*, 2013).

4.2.2 HEMATOPOIETIC STEM CELL TRANSPLANTATION

Before ERT, hematopoietic stem cell transplantation (HSCT) was the only way to treat lysosomal disorders. It employs cells from healthy donors as carriers of the functional enzyme. Cells are supposed to engraft and proliferate in the tissues of patients, including CNS, creating a sub-population able to produce and release the defective enzyme to correct the metabolic defect of the nearby cells. Although HSCT has proven its efficacy in treating some LSDs (Orchard *et al.*, 2007), it only has beneficial effects in a limited number of disorders and it outcomes strongly depend on the severity of the disease and the time of transplantation (Orchard and Tolar, 2010). One example is MPS I in which HSCT is only effective for either intermediate pathology (Hurler syndrome) or when a severe pathology is diagnosed not later than 2.5 years of age. Nevertheless, it remains its first choice of treatment since it improves both clinical manifestation and life expectancy of affected patients (De Ru *et al.*, 2011). Significant limitations of this treatment are also still a significant procedure-related mortality and insufficient engraftment of certain tissues (i.e. bones and heart) and the availability of suitable donors that

may be overcome employing autologous modified HSCs or, though only in part, unrelated donor umbilical cord.

4.2.3 SMALL MOLECULES PHARACOLOGICAL CHAPERONES

As with ERT, small molecule pharmacological chaperones therapy (PCT) is aimed at replacing or increasing the activity of a dysfunctional enzyme. Specifically, it is employed in those LDSs where the loss of the catalytic activity of an enzyme is the result of its abnormal conformation (misfolding). Misfolded proteins are not recognized by the cell and thus not degraded, however, in some cases, the re-acquisition of the right conformation may restore their catalytic activity at least in part. The main advantage of small molecule pharmacological chaperones is their size. They do not require any receptor mediated transport, as they are able to freely diffuse across membrane, including the BBB. Moreover, they can be administrated orally avoiding invasive treatments. One example is 1-deoxygalactonojirimycin (commercially known as Galafold), a physiological inhibitor of α-galactosidase (α-gal) that at low concentration paradoxically acts as its chaperone and increases its activity in patients affected by Fabry disease. The clinical benefits are comparable to those achieved with ERT (Germain and Fan, 2009). Interestingly, chaperones showed the ability to stabilize and even potentiate the activity of recombinant enzymes employed in ERT. In both Pompe disease and Fabry disease the co-administration of PCT and ERT enhanced the intracellular activity of the recombinant enzymes (Flanagan *et al.*, 2009; Porto *et al.*, 2012). The mechanisms through which chaperons can favor the maturation and stability of a wild type exogenous protein are still unclear but in must be independent from any genetic condition. For this reason, the combination of the two treatment can potentially provide benefits to every patient eligible for ERT alone. However, although PCT has already shown clinical efficacy there are some limitation to its

extensive employment for the treatment of LDSs. In fact, one main disadvantage is the impossibility to treat patients indiscriminately since only a fraction of mutations are responsive to chaperone therapy depending on their specific effect on the protein function (Flanagan *et al.*, 2009). Moreover, in most cases, chaperones act as active-site competitive inhibitors, thus at high concentration, may instead inhibit a protein function rather than enhancing it (Parenti, Andria and Valenzano, 2015).

4.2.4 PROTEOSTATIS REGULATORS

Proteostasis involves a variety of biological pathways that regulate protein synthesis and folding, their trafficking and stability and thus, eventually, their degradation. PRs are small drugs able to encourage these intracellular pathways to maintain protein homeostatis. Among these, we find proteasomal inhibitors, heat-shock response (HSR) activators and the so-called “molecular tweezers”.

By inhibiting premature degradation of mutant enzymes, Bortezomib, a proteasomal inhibitors, showed to improve the enzymatic function of multiple lysosomal enzymes mutants of NPC1 with short half-lives. Mutants resulted correctly trafficked to lysosomes and their activity increased leading to lower cholesterol accumulation in NPC fibroblasts (Macías-Vidal *et al.*, 2014).

Similarly, an HSR activator named Calestrol showed promising results in both Gaucher’s and Tay-Sachs affected fibroblasts by increasing the residual activities of both GBA and HEXA. In Gaucher’s cells the treatment also exhibited a synergic effect when combined to N-(n-nonyl)deoxynojirimycin, a PC compound used for the treatment of GD (Mu *et al.*, 2008).

Molecular tweezers are molecules with open cavities capable of binding guest molecules which showed to be particularly effective for those LSDs characterized by amyloidogenic processing mechanisms leading to the progressive formation of insoluble amyloidogenic protein aggregates. Specifically they act by a process-

specific mechanism binding to lysine residues and disrupting molecular interactions that are important for the abnormal self-assembly of multiple amyloidogenic proteins. Among these, CLR01 acts as a broad-spectrum inhibitor of amyloid protein self-assembly reducing lysosomal enlargement and re-activating autophagy. Restoration of the autophagic flux has been associated with reduced neuroinflammation and amelioration of memory deficits in the mouse model of MPS IIIA (Monaco *et al.*, 2020). Up to date, there are no clinically approved PRs for the treatment of LSDs, however several promising compounds in addition to those cited in this paragraph have been identified that can improve the efficacy of therapies for LDSs.

4.2.5 GENE THERAPY

Up to date the most promising treatment for monogenic disease, including LSDs, is gene therapy (GT). Unlike other treatments, GT is based on the delivery of a wild type DNA sequence encoding a specific gene, instead of the missing enzymatic protein, that allows targeted cells to synthetize the functioning protein themselves (Goswami *et al.*, 2019) . The delivery of nucleic acids into a target cell is named “gene transfer” and can be performed through both viral and not viral vectors either *ex vivo*, in cultured cells isolated from the patient and then re-implanted, or *in vivo,* directly into the target tissue of the patient (Goswami *et al.*, 2019a).

Ex vivo gene therapy: Hematopoietic Stem Cell Transplantation

Ex vivo approaches directed at hematopoietic progenitor cells actually demonstrated to be particularly effective for the treatment of some LSDs (Piccolo and Brunetti-Pierri, 2015). Lentiviral vectors (LV) derived from the human immunodeficiency virus type-1 (HIV-1) showed to be particularly suitable for *ex*

vivo GT approaches seen their ability to integrate their genome into that of the host cell but not causing insertional carcinogenesis and the ability to infect both dividing and non-dividing cells (Goswami *et al.*, 2019). LV-engineered hematopoietic stem cells constitutively expressing a therapeutic enzyme showed to be able to migrate to and engraft in different tissues, including CNS where they can transform in microglia, and correct the pathological phenotype in mouse models of metachromatic leukodystrophy (MLD) (Biffi *et al.*, 2004). Similar results were also obtained for Fabry disease (Liang *et al.*, 2007), MPSI (Visigalli *et al.*, 2010), Krabbe disease (Gentner *et al.*, 2010), Pompe disease (Van Til *et al.*, 2010), MPSIIIA (Langford-Smith *et al.*, 2012) and cystinosis (Harrison *et al.*, 2013). *Ex vivo* approaches have two major advantages: they are not invasive and do not require any immunological regulation (i.e. immunosuppression). Currently, two phase I/II studies evaluating safety and efficacy of autologous HSCs treatment for both Hurler syndrome (MPS-I) (ClinicalTrials.gov Identifier: NCT03488394) and San-filippo syndrome (MPSIIIA) (ClinicalTrials.gov Identifier: NCT04201405) are in progress. At the San Raffaele hospital (Milan), pediatric patients are being treated with genetically modified autologous CD34+ hematopoietic stem and progenitor cells transduced with lentiviral vector encoding for the human α-L-iduronidase gene responsible for MPS-I. Concurrently in the United Kingdom, the first human clinical trial to explore the safety, tolerability and clinical efficacy of ex vivo gene therapy in MPSIIIA patients started in January this year. Also in this case, autologous CD34+ cells transduced with a lentiviral vector containing the corrective gene (human SGSH) are being employed.

However, important limitations are still a significant procedure-related mortality and insufficient engraftment of certain tissues (i.e. bones and heart), and there are some concerns about their long-term efficacy and safety. Moreover, *ex vivo* gene

therapy demonstrated to be less effective for the treatment of genetic disorders like inherited metabolic liver diseases (Piccolo and Brunetti-Pierri, 2015).

In vivo gene therapy

In vivo gene therapy demonstrated to be successful for the treatment of several disorders, at least in animal models, and represent the most promising strategy to treat genetic metabolic disorders. Since LSDs affect multiple tissues, actually, many *in vivo* approaches for the treatments of lysosomal disorders are aimed at converting the liver in a stable enzyme-producing factory, not only able to produce the functional enzyme but also to secrete it into the bloodstream and make it available for every other affected tissue as patient's cells are able to take up the circulating protein through M6PR and compensate the enzymatic dysfunction. This way the targeting of a minority of cells can lead to cross-correction of multiple organs and to the rescue of a multisystemic pathology.

Adeno-associated viral (AAV) vectors showed to be the most suitable vectors for GT. Unlike other viral particles, they are nonpathogenic and do not integrate their genome into that of host cells making them a safer solution for gene transfer. Their small size (20nm) allows the crossing of hepatic fenestration, and thus hepatocytes infection, making them particularly suitable for liver gene transfer.

Liver-targeting GT approaches based on AAV intravenous delivery have been successfully employed for the treatment of somatic pathology in different animal models. Specifically, the intravenous administration of AAV vector serotype 8 carrying a liver-specific thyroxine-binding globulin (TBG) promoter driving the expression of the human IDS gene in the mouse model of MPS II completely restored IDS activity in the plasma and tissues of the treated mice. The rescue of the enzymatic activity resulted in the full clearance of the GAGs in all the tissues,

the reduction of GAGs levels in the urine and the correction of the skeleton malformations (Cardone *et al.*, 2006). For MPS VI a phase I/II clinical trial (ClinicalTrials.gov Identifier: NCT03173521) is currently ongoing based on AAV8 with the TBG promoter driving the expression of the human ARSB gene of which administration to MPS VI cats resulted in consistent and dose-dependent expression of ARSB protein, urinary GAGs reduction, and skeletal amelioration (Ferla *et al.*, 2013). Despite these studied demonstrated the ability of AAV intravenous injections to increase the levels of functional enzymes available into the bloodstream, however, the efficient transduction of CNS remains a challenge because of the BBB. One way to overcome this issue is the direct injection of the viral vectors into the CNS. Specifically, direct administration into the CNS represents a suitable delivery strategy when the CNS is the major therapeutic target. It may be achieved by either intracerebral or intrathecal/intraventricular injection in which the therapeutics access the brain, respectively, via parenchyma or via the cerebrospinal fluid. Direct injection of AAV into multiple areas in brain showed a successful increase of enzymatic activity and improved behavioral deficits in preclinical studies on mouse models of MPS IIIA (Motas *et al.*, 2016) and in a canine model of MPS IIIB (Ellinwood *et al.*, 2011). The promising results obtained in preclinical studies led to two clinical trial for both MPS IIIA and MPS IIIB. A phase I/II clinical trial in MPS IIIA patients (Lysogene, ClinicalTrials.gov Identifier: NCT03612869) based on the intracerebral administration of AAV for the delivery of a functional copy of the SGSH gene (Tardieu *et al.*, 2013), and a phase I/II clinical trial in MPS IIIB children (ClinicalTrials.gov Identifier: NCT03300453) based on the intracerebral delivery of the NaGLU gene (Tardieu *et al.*, 2017).

Intra-CSF AAV vector administration also demonstrated to be effective in correcting both somatic and CNS pathology in several lysosomal disorders in

preclinical models. The main advantage of this strategy is the possibility to reach all the CNS structures surrounded by the CSF by injecting the vector in the ventricles or in the subarachnoid spaces filled with the CSF. Moreover, intra-CSF delivery may also target somatic organs due to dispersion of viral vectors into the blood stream. Some examples of intra-CSF injections reporting efficient CNS transduction and rescue of phenotypic aspects came from pre-clinical studied in MPS I (Wolf *et al.*, 2011), MPS IIIA (Haurigot and Bosch, 2013), MPS IIIB (Fu *et al.*, 2010) and MPS VII (Karolewski and Wolfe, 2006) mouse models. Intra-CSF injections combined with systemic delivery of DNA also demonstrated to be effective for the treatment of MSD with a global rescue of the pathological phenotype (Spampanato *et al.*, 2011). It is clear, however, how such an invasive treatment represents an unsuitable solution for patients going into the clinics. For this reason systemic injection via the intravascular route is a noninvasive delivery strategy that represents the elective way to reach peripheral organs and tissues (Fraldi *et al.*, 2018). Sorrentino *et al.* (2013) demonstrated how upon a single intravenous injection of AAV2/8 carrying a chimeric SGSH in which the signal peptide is replaced with that of a highly secreted sulfatase (IDS) performed in adult mouse models of MPS IIIA they were able to efficiently transduce the liver and convert it into a factory for the production of the new chimeric protein. This highly incremented SGSH secretion and consequently its amount available into the blood stream to target every other organ, including the brain (Sorrentino *et al.*, 2013). In addition, brain specific targeting was achieved by the addition of a second peptide at the c-terminus of SGSH, the Apolipoprotein B binding-domain (ApoB-BD) sequence. This in order to induce a receptor-mediated transcytosis of the enzyme in the cells of the BBB via the low-density lipoprotein receptor (LDLR). Their results showed an overall improvement of brain pathology demonstrated by reduced vacuolization, re-establishment of the normal autophagic flux and

reduction of inflammation signs. The recovery of a normal behavioral phenotype was observed in affected mice and thus the ability of the treatment to induce protein levels high enough to treat brain pathology was further confirmed (Sorrentino *et al.*, 2013).

The main advantage of gene therapy compared to other treatments is the potential long-term expression of the therapeutic protein. However, the clinical translation of this approach is very challenging due to the difficulty in achieving and maintaining therapeutic threshold levels of the corrective enzyme in targeted tissues avoiding potential toxic effects caused by high dosage and/or repeated administration of the viral vectors used for gene delivery. Moreover, immune response represents one main obstacle to viral infection, specifically pre-existing immunity against AAV capsids that can neutralize viral particles from circulation. In addition, the episomal nature of recombinant AAV genomes can be a limitation for gene transfer in dividing cells since cell division causes dilution of viral genomes. This is particularly relevant for the liver, resulting in the limitation of applicability of in vivo GT approaches in paediatric age and the reduction of its efficacy in the case of a post-treatment liver injury.

Genome editing

The last decades has seen Genome Editing (GE) arise as an exciting approach for the treatment of inherited diseases. Its main objective is to correct the function of defective genes by modifying the genome of the affected cells with the highest possible precision. Genome engineering tools typically induce DNA double-stranded breaks at a specific target locus and exploit endogenous cellular repair pathways to introduce specific exogenous therapeutic DNA sequences. Among the different GE technologies available up to date, in vivo studies have been

performed employing zinc-finger nucleases (ZFNs), transcription activator-like effector nucleases (TALENs) and the CRISPR-Cas9 (clustered regularly interspaced short palindromic repeats/caspase 9) system (Jessica L. Schneller *et al.*, 2017).

Specifically, several pre-clinical studies have been conducted to investigate the efficiency of CRISPR-Cas9 based therapeutic approaches for several diseases like Duchenne Muscular Dystrophy, Retinitis Pigmentosa and Hereditary Tyrosinemia type I (Ho *et al.*, 2018). Different strategies have been investigated during the years to improve both the efficacy and safety of the technique and eventually lead to clinical studies. Sangamo BioSciences is currently exploring therapeutic strategies based on targeted insertion of the functional gene at the albumin locus in hepatocytes through in-vivo ZFN-mediated genome editing for MPS I (ClinicalTrials.gov Identifier: NCT02702115) and MPS II (ClinicalTrials.gov Identifier: NCT03041324) in two phase I/II studies. Both the therapeutics are delivered by adeno-associated virus (AAV) vectors. The placement of the corrective copy of respectively human IDUA and IDS transgenes under the control of the highly expressed endogenous albumin locus is expected to provide permanent, liver-specific expression of the target defective enzymes for the lifetime of affected patients. No data have jet been published about the trial's outcome. Despite the very promising results and the huge potential that genome editing and the CRISPR-Cas9 system have for the specific life-long correction of genetic defects, there are still concerns about its long-term safety. The risk of generating secondary mutations (off-targets) it is not to be overlooked (Schaefer *et al.*, 2017), therefore, more studies are needed to further validate the reliability of the technique before it can be actually employed in humans.

4.2.6 SUBSTRATE REDUCTION THERAPY

Substrate-reduction therapy (SRT), also known as “substrate deprivation”, is a specific drug therapy based on the inhibition of substrate synthesis to prevent their accumulation within cells. It employs small-molecules able to interfere with specific steps of the biosynthetic pathways of different types of substrates. For example, the use of N-butyldeoxynojirimicin (Miglustat) has been already approved (commercial name Zavesca) as treatment for Gaucher’s disease (Futerman *et al.*, 2004) and NPC (Patterson *et al.*, 2007), both characterized by the accumulation of glycosphingolipids. Miglustat acts on glucosylceramide synthase, the first enzyme in the biosynthetic pathway of glycolipids in the Golgi (Platt *et al.*, 1994). This way the balance between synthesis and degradation of sphingolipids is partially restored limiting their accumulation within lysosomes (Platt and Jeyakumar, 2008). Like other small-molecules, Miglustat has the major advantage of being able to cross the BBB and demonstrated its efficacy in stabilizing the neurological disease in NPC patients (Patterson *et al.*, 2007). In addition, it can be administrated orally and do not require immunological modulation. For these reasons it is a suitable candidate for the treatments of all the sphingolipidoses, in particular those characterized by CNS pathology. A main advantage of SRT treatments is indeed the possibility to employ a single molecule in the treatment of an entire class of diseases where aggregates share the same biosynthetic pathways.

5. AIMS

5.1 Rationale of the research project

Enzyme and gene/cell replacement strategies aimed at correcting defective hydrolytic lysosomal protein represent the first and the most promising option for the treatment of LSDs. However, the effective clinical application of these protocols is particularly challenging. A major reason is the difficulty in achieving and maintaining therapeutic threshold levels of the corrective enzyme in targeted tissues, particularly in the brain, avoiding potential toxic effects caused by high dosage and/or repeated administration of therapeutic enzymes or vehicles.

In contrast to loss-of-function mutations in lysosomal enzymes, responsible for disease conditions, there are a number of examples of naturally occurring gain-of-function (GOF) mutations in hydrolytic enzymes that enhance their stability and/or intrinsic catalytic activity and that have been used for therapeutic purposes. Ross et al. (2004) demonstrated the possibility to treat the Lipoprotein lipase deficiency (LPLD) in LPL-deficient mice in a pre-clinical gene therapy study employing a naturally occurring gain-of-function LPL variant with increased lipolytic function (Ross *et al.*, 2004). Clinical trials were later conducted on LPLD patients using the same strategy (Stroes *et al.*, 2008; Gaudet *et al.*, 2013). Similarly, the administration AAV vectors encoding a hyperactive variant of factor IX in both hemophilia B (HB) dog and mouse models showed promising results for the treatment of HB supporting the potential translation of gene-based strategies using GOF enzymes (Crudele *et al.*, 2015).

The possibility of generating GOF versions of enzymes “ad hoc” may greatly improve replacement therapeutic protocols for the treatment of LSDs. Such “hyperactive” proteins may be employed in gene transfer approaches based on their enhanced activity to produce a beneficial effect in targeted tissues,

particularly in the brain, at much lower doses and more efficiently compared to the respective wild type enzymes.

5.2 Specific Aims

The aim of my PhD project was to develop and set up a high-throughput functional screening tool to identify lysosomal enzyme variants carrying GOF mutations that enhance the catalytic activity and/or the stability of the enzyme.

The ultimate goal is to generate lysosomal enzymes with improved therapeutic potential. This method has been validated and applied to three different lysosomal enzymes:

- The β-glucosylceramidase (GBA), which is defective in Gaucher disease
- The β-galactosidase (GLB1), which is defective in GM1-gangliosidosis and Morquio B syndrome
- The β-glucuronidase (GUSB), which is defective in Mucopolysaccharidosis type VII

6. MATERIALS AND METHODS

6.1 Generation of pLVX-EF1a-p2A.m-Cherry-PURO vectors

The p2A-mCherry sequence was amplified from the pP2A-mCherry-N1 vector (Addgene plasmid #84329) using a forward primer

5'- TCCTCGAGACTAGTTCTAGAGGATCGGGTGCTACTAACTTCAGCC -3'

containing a XbaI restriction sequence and part of the p2A sequence at the 3' end, and a reverse primer

5'- GAGGGAGAGGGGCGGGATCCTTACTTGTACAGCTCGTCCATGCC -3'

containing the c-term sequence of mCherry tag including a STOP codon and a BamHI restriction sequence.

The PCR product was resolved on a 1% agarose gel and then purified using the QIAquick Gel Extraction kit (Quiagen, Milan, Italy) to be ligated into the pLVX-EF1α-IRES-Puro vector. Ligation was performed using the In-Fusion HD Cloning Kit (Takara, Shiga, Japan) according to manufacturer's protocols. The ligation product was transformed into Stellar™ competent cells (Takara, Shiga, Japan) and selected on ampicillin-containing LB agar plates at 37° for 18h. Multiple colonies were then collected and expanded in ampicillin-containing LB medium and plasmid DNA extracted using the Quiagen Miniprep kit (Quiagen, Milan, Italy). Control digestion using XbaI and BamHI restriction enzymes were performed in order to confirm the success of the cloning procedure and select one colony to be further expanded in ampicillin-containing LB medium and plasmid DNA extracted using the Quiagen Midiprep kit (Quiagen, Milan, Italy).

6.2 Generation of hGBA, hGUSB and hGLB1 pLVX-EF1a-p2A.m-Cherry-PURO vectors

Each sequence was amplified using specific forward primers:

GBA 5'- TTCCTCGAGACTAGTTCTAGAATGGAGTTTTCAAGTCCTTCCAG -3'

GUSB 5'- TTCCTCGAGACTAGTTCTAGAATGGCCCGGGGGTCGGCG -3'

GLB1 5'- TTCCTCGAGACTAGTTCTAGAATGCCGGGGTTCCTGGTT -3'

overlapping the pLVX-EF1a-p2A.m-Cherry-PURO vector at the 5' end, and a common reverse primer

5'- AGTAGCACCCGATCCTCTAGACTTATCGTCGTCATCCTTGTAATC -3'

containing part of the p2A sequence at the 3' end. All the primers contained a XbaI restriction sequence.

The PCR product was resolved on a 1% agarose gel and then purified using the QIAquick Gel Extraction kit (Quiagen, Milan, Italy) to be ligated into the pLVX-EF1α-p2A m-Cherry-IRES-Puro vector. Ligation was performed using the In-Fusion HD Cloning Kit (Takara, Shiga, Japan) according to manufacturer's protocols. The ligation product was transformed into Stellar™ competent cells (Takara, Shiga, Japan) and selected on ampicillin-containing LB agar plates at 37° for 18h. Multiple colonies were then collected and expanded in ampicillin-containing LB medium and plasmid DNA extracted using the Quiagen Miniprep kit (Quiagen, Milan, Italy). Control digestion using XbaI restriction enzyme were performed in order to confirm the success of the cloning procedure and select one colony to be further expanded in ampicillin-containing LB medium and plasmid DNA extracted using the Quiagen Midiprep kit (Quiagen, Milan, Italy).

6.3 Cell lines culture conditions

GUSB-KO mouse embryonic fibroblasts (MEF) were maintained in DMEM supplemented with 20% FBS supplemented with 1% L-glutamine and 1% Penicillin-Streptomycin solution (Pen/Strep) (Gibco, Thermo Fisher Scientific, Waltham, MA, USA).

GBA-KO MEFs were maintained in DMEM supplemented with 10% FBS supplemented with 1% L-glutamine and 1% Pen/Strep (Gibco, Thermo Fisher Scientific, Waltham, MA, USA).

Human foreskin fibroblasts (HFF) were maintained in DMEM supplemented with 15% FBS supplemented with 1% L-glutamine and 1% Pen/Strep (Gibco, Thermo Fisher Scientific, Waltham, MA, USA).

Human gangliosidosis type 1 (GM1) fibroblasts were maintained in DMEM supplemented with 20% FBS supplemented with 1% L-glutamine and 1% Pen/Strep (Gibco, Thermo Fisher Scientific, Waltham, MA, USA).

6.4 Western Blotting

Cell pellets were homogenized in ice-cold 3Xflag lysis buffer 1X (50mM Tris-HCl pH 8, 200mM NaCl, 1% Triton X100, 1mM HEPES) in presence of protease inhibitors (Sigma-Aldrich, MO, USA) 1:200. Lysates were obtained by 30 mins incubation in lysis buffer on ice and then centrifuged at maximum speed for 10 min to eliminate cellular debris. Protein concentration was determined using the Bio-Rad (Bio-Rad, Hercules, CA, USA) colorimetric assay.

Protein (20 µg) were prepared in FBS sample buffer 6X. Samples were then boiled at 90°C for 3 min and resolved onto 10% mini protean SDS-PAGE gels at constant voltage (100V) for about 1,5h at room temperature (RT) against a Pre-stained Protein Standard (11-245 kDa) (New English Bioscience, MA, USA). Proteins were transferred from SDS-PAGE gels to PVDF membranes (Millipore, MA, USA) at constant voltage (110V) for 1h at 4°C. Transfer membranes were blocked in 5% Milk-PBS-0.1% Tween (PTW) for 1h at RT and, afterwards incubated in primary antibody (5% Milk-PTW) O/N at 4°C. The following day membranes were washed in PTW (3x 10 mins) before 1h secondary antibody incubation (in 5% Milk-PTW) and further washed in PTW (3x 10 mins). Primary and secondary antibodies employed are listed in the table below (Table 2).

Antibody	Species	Dilution	Company
Flag (HRP)	Mouse	1:1000	Sigma
mCherry	Mouse	1:1000	Abcam
Anti-Mouse secondary antobody	Rabbit	1:5000	Calbiochem

Table 2. Antibodies used for western blotting analysis.

6.5 Generation of Gain-of-Function and Loss-of-Function mutants of GUSB

GUSB mutants were obtained by amino acid substitutions by site-directed mutagenesis using the Quik Change II XL Site directed Mutagenesis kit (Agilent Technologies, Santa Clara, CA, USA). Specifically, to generate the Gain-of-Function (GOF) variant of GUSB amino acidic substitutions were singularly and sequentially performed in positions 243 (Leu→Gln), 255 (Leu→Gln) and 545 (Thr→Gly). While, for the Loss-of-Function (LOF) variant one single amino acid substitution was performed in position 508 (Tyr→Cys). The oligos used for the mutagenesis are listed in the table below (Table 3).

Position	AA substitution	Direction	Sequence
243	Leu→Gln	forward	5'-GCAAGACAGTGGGCAGGTGAATTACCAGAT -3'
243	Leu→Gln	reverse	5'- ATCTGGTAATTCACCTGCCCACTGTCTTGC -3'
255	Leu→Gln	forward	5'- CAAGGGCAGTAACCAGTTCAAGTTGGAAGT -3'
255	Leu→Gln	reverse	5'- ACTTCCAACTTGAACTGGTTACTGCCCTTG -3'
545	Thr→Gly	forward	5'- AGTATGGAGCAGAAGGGATTGCAGGGTTTC -3'
545	Thr→Gly	reverse	5'- GAAACCCTGCAATCCCTTCTGCTCCATACT -3'
508	Tyr→Cys	forward	5'- CTACTACTCTTGGTGTCACGACTACGGGCA -3'
508	Tyr→Cys	reverse	5'- TGCCCGTAGTCGTGACACCAAGAGTAGTAG -3'

Table 3. Oligo pairs used for site-directed mutagenesis of GUSB. In red the nucleotides substitutions necessary to generate the amino acidic substitutions.

6.6 Generation of randomly mutagenized GBA libraries

Error-prone PCR

The pLVX-EF1a-GBA-p2A-mCherry-IRES-PURO vector was employed as a template for error-prone PCR using the IN-fusion designed primers previously employed to generate the vector itself. Each 50µl PCR reaction contained 1µl of mutagenic buffer (10mM dCTP, 10mM dTPC, $MgCl_2$ 1M, $MnCl_2$ 1M) and was amplified using 5 units of Taq polymerase (Takara, Shiga, Japan).

Generation of GBA pLVX libraries

Error-prone PCR products were resolved on a 1% agarose gel and then purified using the QIAquick Gel Extraction kit (Quiagen, Milan, Italy) to be ligated into the pLVX-EF1α-p2A m-Cherry-IRES-Puro vector by using the In-Fusion HD Cloning Kit (Takara, Shiga, Japan) according to manufacturer's protocols. Multiple ligation reactions were performed in order to employ the entire volume of the PCR

products. For each gene, the ligation products were pooled together and transformed into Stellar™ competent cells (Takara, Shiga, Japan). 10µl of each pool were selected on ampicillin containing LB agar plates at 37° for 18h. The resulting colonies were counted to evaluate the total number of possible colonies and thus the complexity of the mutants libraries. The remaining amount was selected and expanded in ampicillin containing LB medium and plasmid DNA extracted using the Quiagen Miniprep kit (Quiagen, Milan, Italy).

The resulting plasmids were used to generate corresponding Lentiviral libraries.

6.7 Fluorescence-activated Cell-Sorting (FACS) Analysis

Cells were plated and transfected 24h later using Lipofectamine 3000 (Invitrogen S.R.L., Milam, Italy), according to manufacturer's protocols, with pLVX-EF1a-GUSB-p2A-mCherry-IRES-PURO or pLVX-EF1a-GBA-p2A-mCherry-IRES-PURO plasmids. 24h after transfection synchronization was induced by replacing standard medium with DMEM supplemented with Thymidine (Sigma-Aldrich, MO, USA) at a final concentration of 2mM. 48h after transfection Thymidine-supplemented medium was removed and cells incubated with 250µM either C12-Di-β-D-Glucoronide (Vinci Biochem, Vinci, Florence, Italy) or C12-Di-β-D-Glucopyranoside (Vinci Biochem, Vinci, Florence, Italy) or C12-Di-β-D-Galactopyranoside (C12FDG) (Invitrogen, Thermo Fisher Scientific, Waltham, MA, USA) at 37° for 1h.

Cells were detached with trypsin 0.05% EDTA (Thermo Fisher Scientific, Waltham, MA USA) and resuspended in sorting solution containing PBS, 5% FBS and 2.5mM EDTA. Cells were analysed on a BD FACS ARIA III (BD Biosciences, San Jose, CA, USA) equipped with BD FACS Diva software (BD Biosciences) using

appropriate excitation and detection settings for red and green fluorescence. Thresholds for fluorescence detection were set on untransfected cells, and a minimum of 10,000 cells/sample were analysed. When necessary Green+/mCherry+ cells were sorted and cultured to be expanded for following analysis.

6.8 Lentiviral infection

The basic conditions for the viral transduction procedure were common to all the viral prep and cell lines employed.

Cultured cells were dissociated with trypsin-EDTA (Thermo Fisher Scientific, Waltham, MA USA) counted and resuspended in antibiotic-free medium supplemented with inactivated FBS (at 55°, 30 mins) and polybrene (Sigma-Aldrich, MO, USA) at concentration of 4 µg/ml. Cells were then infected in suspension with a multiplicity of infection (MOI) of 64 (to determine the optimal MOI for MEF cells MOIs from 0.5 – 128 were tested). Cells were plated in the infection volume and incubated at 37° for 16h. The number of cells and volume of infection were adjusted according to the plate employed for each experiment.

6.9 Genomic DNA extraction and purification

To extract genomic DNA (gDNA) cell pellets were lysed in 450µl of lysis buffer (50mM TRIS HCl Ph 8.0, 100mM EDTA, 100mM NaCl, 1%SDS) and 450µl of phenol-clorophorm solution were added to the cell lysate. The solution was then spinned for 1 min at 20.000xg, the supernatant was harvested and 2.5 volumes of cold 100% ethanol (Et-OH) were added. The solution wsa then centrifuged for 20

mins at 18.000xg. The resulting pellet was washed with 1ml of 80% Et-OH and centrifuged again for 10 mins. It was allowed to dry at RT and then resuspended in 50µl of TE buffer. 100µl of Ampure beads were added to DNA and incubated for 10 mins on a magnetic rack to purify the extracted gDNA. The supernatant was removed and the pellet washed twice with 80% Et-OH. The tube was then removed from the magnetic rack and the pellet was allowed to air-dry. The beads were then resuspended in 15µl of H2O and incubated for 5 mins and then for additional 5 mins on a magnetic rack. gDNA was recovered in the supernatant and quantify by qubit.

6.10 Viral DNA (vDNA) preparation

After virus preparation, RNA was extracted from 100uL of viral suspension (concentrated with PEG 1:100) with *Quick*-RNA Miniprep Plus Kit, and eluted in 35µL of RNAse-free water. REtrotranscription was performed using the SuperScript™ IV VILO™ Master Mix with ezDNase™ Enzyme following the protocol with 8uL with a final volume of 20µl.

6.11 GBA library preparation

Twenty oligo pairs were deigned to amplify the entire GBA gene sequence by overlapping fragments of ~100bp. The oligos were pooled together to perform a multiplex PRC reaction using KAPA HIFI polymerase on both gDNA and vDNA. Oligos are listed below (Table 4).

Oligo ID	Sequence
GBA_seq_Fw1	5'- ATGGAGTTTTCAAGTCCTTC -3'
GBA_seq_Fw2	5'- CACAGGATTGCTTCTACTTC -3'
GBA_seq_Fw3	5'- CGGTGGTGTGTGTCTGCAATG -3'

GBA_seq_Fw4	5’- CAGCCGCTATGAGAGTACAC -3’
GBA_seq_Fw5	5’- CTACTGACCCTGCAGCCAGAA -3’
GBA_seq_Fw6	5’- GCTGCTCTCAACATCCTTGC -3’
GBA_seq_Fw7	5’- ACATCATCCGGGTACCCATG -3’
GBA_seq_Fw8	5’- GATGATTTCCAGTTGCACAA -3’
GBA_seq_Fw9	5’- CAGCGTCCCGTTTCACTCCT -3’
GBA_seq_Fw10	5’- GGTGAATGGGAAGGGGTCACT -3’
GBA_seq_Fw11	5’- GCTGAGCACAAGTTACAGTT -3’
GBA_seq_Fw12	5’- GTGGATACCCCTTCCAGTGC -3’
GBA_seq_Fw13	5’- CTCACCACAATGTCCGCCTA -3’
GBA_seq_Fw14	5’- GACCCAGAAGCAGCTAAATA -3’
GBA_seq_Fw15	5’- GGAGACACACCGCCTGTT -3’
GBA_seq_Fw16	5’- CAGAGTGTGCGGCTAGGCTC -3’
GBA_seq_Fw17	5’- GCTGGACCGACTGGAACCTT -3’
GBA_seq_Fw18	5’- CATCATTGTAGACATCACCA -3’
GBA_seq_Fw19	5’- TCCCAGAGAGTGGGGCTGGTT -3’
GBA_seq_Fw20	5’- GGCTCTGCTGTTGTGGTCGT -3’
GBA_seq_Rv1	5’- GTAGCCGAAGCTTTTAGGGA -3’
GBA_seq_Rv2	5’- GTACCAAGGGCAGGAAAGGT -3’
GBA_seq_Rv3	5’- GTGCCCGTGTGATTAGCCTG -3’
GBA_seq_Rv4	5’- TCTGTCATGGCCCCTCCAAA -3’
GBA_seq_Rv5	5’- TCCGATTCCTTCTTCAGAGA -3’
GBA_seq_Rv6	5’- GGTGTCTGCATAGGTGTAGG -3’
GBA_seq_Rv7	5’- CAACTGCAGGGCTCGGTGAA -3’
GBA_seq_Rv8	5’- CCATTGGTCTTGAGCCAAGT -3’
GBA_seq_Rv9	5’- GCATCCAGGAACTTCACAAA -3’
GBA_seq_Rv10	5’- CAGCCCAGCAGAAGGCTCAT -3’
GBA_seq_Rv11	5’- GTTGGCGAGGGTAGGACCTA -3’
GBA_seq_Rv12	5’- GTACCACCTTTGCCCAGTGG -3’
GBA_seq_Rv13	5’- CTTTGGCTGGAGCCAGAAAG -3’
GBA_seq_Rv14	5’- GAACTTGGAGCCCACACAGG -3’
GBA_seq_Rv15	5’- CATGGTACAGGAGGTTCGTG -3’
GBA_seq_Rv16	5’- GTCGACAAAGTTACGCACCC -3’
GBA_seq_Rv17	5’- GAATGAACTTGCTGAAGTGG -3’
GBA_seq_Rv18	5’- GGATGCATCAGTGCCACTGC -3’
GBA_seq_Rv19	5’- CACAGCAGGATCCTTGATGG -3’
GBA_seq_Rv20	5’- TCACTGGCGACGCCACAGGTA -3’

Table 4. Oligo pairs used for the amplification of GBA fragments. Fw= forward, Rv= reverse.

The PCR products were purified using Ampure beads, as previously described, and resolved on 2% gel. DNA fragments were extracted from gel and eluted in 10µl H_2O.

The GBA library was prepared through the NEBNext® Ultra™ II DNA Library Prep Kit for Illumina® QC library (tapestation) (Illumina, San Diego, California, USA) and sequenced on Miseq with V3 150cycles flowcell (Illumina, San Diego, California, USA).

6.12 Reads quality check, trimming and alignment

Reads were checked for quality using FastQC (Andrews, 2010) (version 0.10.1). Subsequently, adapters removal and quality trimming were performed by Trim Galore (Krueger, 2016) (version 0.4.1) with default parameter and setting the minimum read length after trimming to 120bp. The alignment to the reference sequence of GBA has been performed by Bowtie2 (Langmead and Salzberg, 2013) (version 2.3.2) with default parameters and the outputted SAM file was converted to BAM using samtools (Li *et al.*, 2009) (version 1.3).

6.13 Mutational load and comparative analysis

To evaluate the mutational load in each sample, we addressed the recurrence of mismatches in each aligned read using the output of sam2tsv, one of the tools from JVarkit (Lindenbaum, 2015). Once these values have been obtained, synonym mutations were filtered out and the remaining ones normalized by the total number of input reads. Finally, the score was evaluated by comparing the normalized value of a mutation in a sample against the normalized value of the same mutation in the viral library.

6.14 Enzymatic activity assays

Cell samples were mechanically lysed by 4 cycles of freeze/thaw and then centrifuged at 10.000 rpm to recover the supernatants. Protein concentration was determined using the Bio-Rad colorimetric assay (Bio-Rad, Hercules, Ca, USA). To measure enzymes activity 10µg of total protein extract were incubated with the relative 4-methylumbelliferyl-substrates (4-MU): 4-MU-β-D-glucuronide, 4-MU-β-D-glucopyranoside (Sigma-Aldrich, MO, USA) at 37˚C. The reaction was then stopped with 100µl of stop buffer and the processed 4-MU measured using 365nm excitation and 460nm emission in the Promega GloMax fluorimeter (Promega, Madison, WI, USA). Protein and substrates concentration, time of incubation and composition of stop solutions are reported in the table below (Table 5).

Enzyme	Final concentration of substrate	Time (h)	Stop solution
GUSB	5mM	1	0.5M $NaHCO_3$/0.5M Na_2CO_3, pH 10.7
GBA	3mM	2	15mM EDTA/3M glycine, pH 10.3

Table 5. 4-MU assay specific protocols for GUSB and GBA.

6.15 Sequencing analysis of cellular clones

gDNA was extracted from each cell pellets through phenol-chloroform protocol and the GBA sequences specifically amplified by PCR. The following oligos were used:

genomicGBA forward 5'- TCGAGACTAGTTCTAGAATG -3'

genomicGBA reverse 5'- AGCAGGCTGAAGTTAGTAGC -3'

DNA sequencing analysis were performed on the resulting PCR products by Eurofins Genomics GmbH, Ebersberg, Germany. The amplifying oligos were also employed as sequencing primers, but two additional sequencing primers were

used in order to cover the entire 1500bp sequence given the company requirement for efficient sequencing. The additional sequencing primers are listed below:

GBAseq forward 5'- GGGCCAGATACTTTGTGAAG -3'

GBAseq reverse 5'- CTTCACAAAGTATCTGGCCC -3'

6.16 Generation of customized GBA mutants libraries

DNA oligo (200bp) library pools were purchased from Agilent (Santa Clara, CA, USA) as single-strand sequences. To generate double-strand DNA, all the sequences, within the same library, were designed with common terminal sequences to be used as annealing sites for a PCR reaction. The oligos employed for the library amplification are listed in the table below (Table 6).

Library	Direction	Sequence
POOL_1	forward	5'- CTGGGCAGTGAC AGC TGA A -3'
POOL_1	reverse	5'- CCTTTGCCCAGT GGG GCA GC -3'
POOL_2	forward	5'- CCTTTGCCCAGT GGG GCA GC -3'
POOL_2	reverse	5'- GCCGCACACTCT GCT CCC AG -3'

Table 6. Oligo pairs used for the amplification of customized GBA libraries.

6.17 Generation of site-directed mutations for GBA

GBA mutants were produced as previously describe (paragraph 6.5). Specifically, nucleotide substitutions were singularly and/or sequentially performed in positions 380 (C→T), 1216 (A→G), 1238 (A→T), 1328 (A→T), 1334 (T→A), 1340 (A→C) and 1341 (G→C), 712 (G→A), 850 (C→G) and 1141 (T→A). The oligos used are listed in the table below (Table 7).

Position	Nucleotide substitution	Direction	Sequence
380	C→T	forward	5’- GCCATGACAGATGTTGCTGCTCTCAACATC -3’
380	C→T	reverse	5’- GATGTTGAGAGCAGCAACATCTGTCATGGC -3’
1216	A→G	forward	5’- AGTACAGCCACAGCGTCATCACGAACCTCC -3’
1216	A→G	reverse	5’- GGAGGTTCGTGATGACGCTGTGGCTGTACT -3’
1238	A→T	forward	5’- GAACCTCCTGTACCTTGTGGTCGGCTGGAC -3’
1238	A→T	reverse	5’- GTCCAGCCGACCACAAGGTACAGGAGGTTC -3’
1328	T→C	forward	5’- CAGTCCCATCATTGCAGACATCACCAAGGA -3’
1328	T→C	reverse	5’- TCCTTGGTGATGTCTGCAATGATGGGACTG -3’
1334	T→A	forward	5’- CATCATTGTAGACAACACCAAGGACACGTT -3’
1334	T→A	reverse	5’- AACGTGTCCTTGGTGTTGTCTACAATGATG -3’
1340	A→C	forward	5’- TGTAGACATCACCACGGACACGTTTTACAA -3’
1340	A→C	reverse	5’- TTGTAAAACGTGTCCGTGGTGATGTCTACA -3’
1341	G→C	forward	5’- TGTAGACATCACCAACGACACGTTTTACAA -3’
1341	G→C	reverse	5’- TTGTAAAACGTGTCGTTGGTGATGTCTACA -3’
712	G→A	forward	5’- AGGGGTCACTCAAGAGACAGCCCGGAGACA -3’
712	G→A	reverse	5’- TGTCTCCGGGCTGTCTCTTGAGTGACCCCT -3’
850	C→G	forward	5’- TGTTGAGTGGATACGCCTTCCAGTGCCTGG -3’
850	C→G	reverse	5’- CCAGGCACTGGAAGGCGTATCCACTCAACA -3’
1141	T→A	forward	5’- TTGCCTCAGAGGCCAGTGTGGGCTCCAAGT -3’
1141	T→A	reverse	5’- ACTTGGAGCCCACACTGGCCTCTGAGGCAA -3’

Table 7. Oligo pairs used for site-directed mutagenesis of GBA. In red the nucleotides substitutions necessary to generate the mutations

7. RESULTS

7.1 Design of the functional selection tool to screen GOF variants of lysosomal hydrolases based on fluorescence-activated cell sorting (FACS)

To identify gain-of-function (GOF) variants of lysosomal hydrolases I developed a high-throughput method based on fluorescence-activated cell-sorting (FACS) that allows the screening and selection of enzymes hyperactive variants in physiological conditions. As outlined in figure 2 this method employs optimized intra-vital fluorogenic substrates to specifically label (FL1 in figure 2) the catalytic activity of lysosomal hydrolases in living cells and cleavable mCherry fluorescent tag to label (FL2 in figure 2) the expression levels of the specific lysosomal hydrolase. Error-prone PCR is used to generate randomly mutagenized cDNAs of the specific lysosomal hydrolase. Lentiviral-derived libraries containing mutated hydrolase variants tagged with mCherry are used to express the enzyme variants in cultured cells. Cells exhibiting enhanced enzymatic activity are then sorted by FACS as they potentially correspond to those expressing GOF variants. At this point there are two different possible approaches to identify putative gain-of-function mutants. The first completely unbiased approach consists in the recovery of gDNA from sorted cells and a deep sequencing analysis to identify mutations enriched in the selected population since highly enriched mutations within a selected cell sub-population are more likely to be responsible for the population phenotype (in this case increased enzymatic activity). Otherwise, sorted cells can be cultured and expanded to generate clones originating from single cells and later collected to perform enzymatic activity assay. This way it is possible to specifically identify those clones expressing increased enzymatic activity, collect their DNA

and, through Sanger sequencing analysis, identify the specific mutations responsible for the increased enzymatic activity (Figure 2).

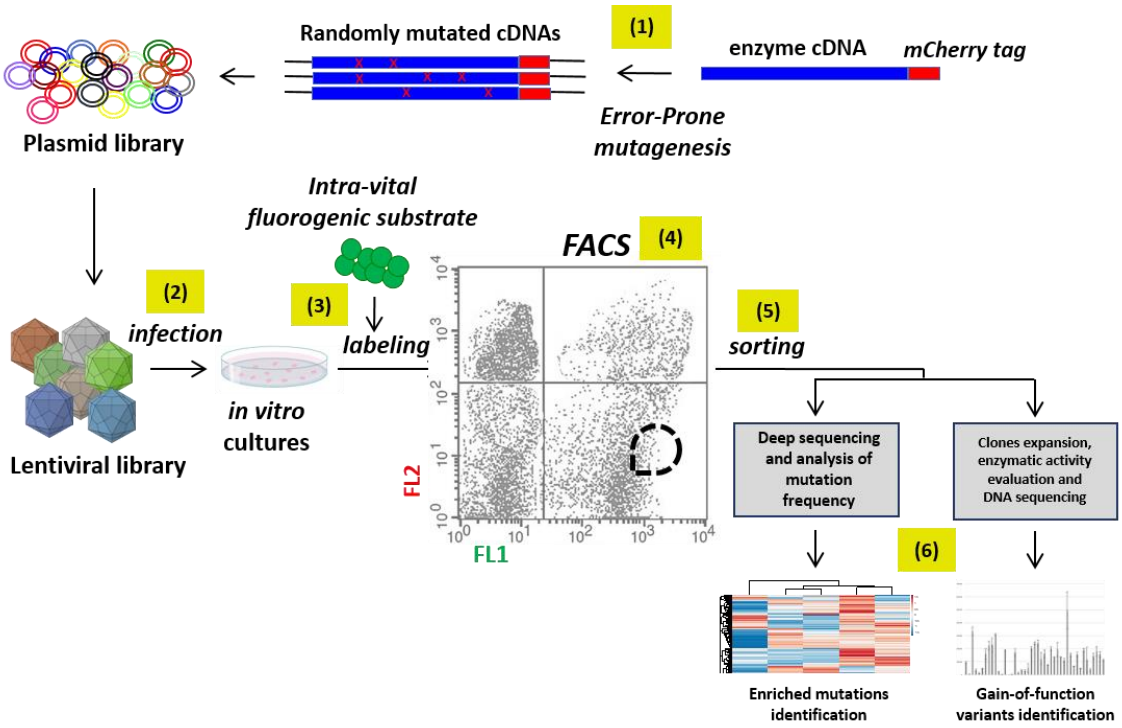

Figure 2. Outline of the functional selection method. (1) Error-prone PCR to generate randomly mutagenized cDNAs of the specific lysosomal hydrolase. (2) Generation of lentiviral-derived libraries to infect cultured cells (lacking the specific enzymatic activity analysed) with mutated enzymes. Multiplicity of infection (MOI) will be adjusted to maximize the probability that one cell is infected by one viral particle. (3) Optimized intra-vital fluorogenic substrates to specifically label (FL1) in a very sensitive manner the catalytic activity of lysosomal hydrolases in living infected cells. (4) mCherry fluorescent tag sequence to label (FL2) the expression levels of the specific lysosomal hydrolase in infected cells (the tool employs a self-cleaving enzyme-mCherry fusion protein to preserve enzyme folding). (5) FACS to sort cells exhibiting enhanced enzymatic activity (FL1) relative to enzyme expression levels (FL2). (6) Collection and/or amplification of sorted cells, recovery of mutated gDNAs and sequencing analysis.

7.2 Generation of fluorogenic intra-vital substrates for lysosomal hydrolases

To make such FACS-based tool working it was crucial to obtain a fluorogenic substrate capable to quantitatively and sensitively label the specific lysosomal enzymatic activity in intact cells. To generate such substrate I employed the 5-Dodecanoyl-amino-fluorescein (C12), a green fluorescent lipophilic fluorophore

that remains associated within cells and is therefore suitable for flow cytometry analysis (Kurz *et al.*, 2000) (Figure 3).

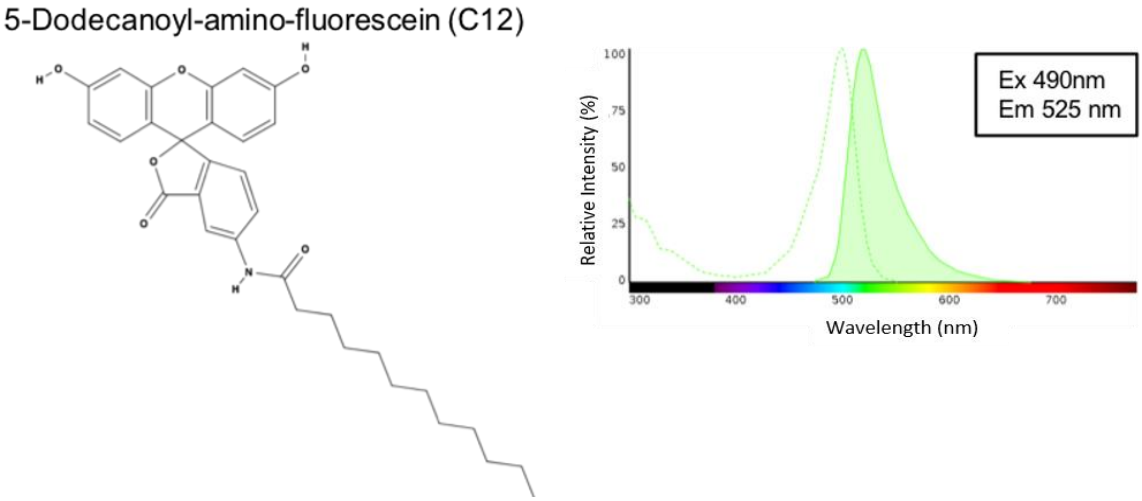

Figure 3. The molecular structure of 5-Dodecanoyl-amino-fluorescein (C12). The lipophilic fluorophore is shown along with its fluorescence spectra (C12 emits green fluorescence upon excitation at 490 nm).

Intra-vital fluorogenic substrates were produced for three different lysosomal enzymes: β-glucuronidase (GUSB), β-glucosylceramidase (GBA) and β-galactosidase (β-gal). They were generated by coupling the C12 molecule with the enzyme native substrates, respectively glucuronide, glucopyranoside and galactopyranoside sugars (Figure 4).

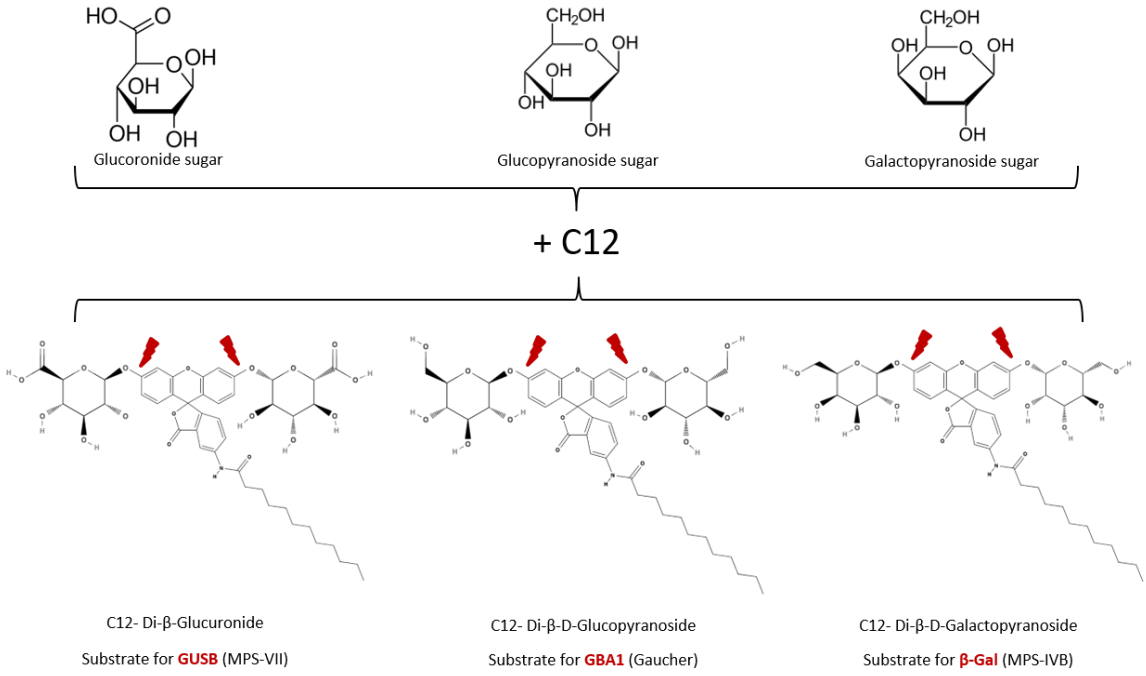

Figure 4. C-12 derived intra-vital fluorogenic substrates for GUSB, GBA1 and β-Gal enzymes. Glucoronide, glucopyranoside and galactopyranoside sugars were coupled to the C12 moiety to generate the respective fluorogenic substrates: C12-Di-β-D-Glucoronide, C12-Di-β-D-Glucopyranoside or C12-Di-β-D-Galactopyranoside.

It was possible to produce these specific substrates as the biochemical properties of C12 only allow it to be bound to monomeric sugars through a beta-glycosidic bond and therefore to those sugars which are normally linked together through beta-glycosidic bonds.

The C12 derived substrates are membrane permeable and are able to enter the cell thanks to their polar component composed of the sugars that constitute the substrate for lysosomal enzymes, however, upon hydrolysis, the C12 fluorophore precipitate thus remaining confined within the cells being not able to exit anymore. Moreover, when coupled with sugar residues the C12 is not fluorescent thus C12-derived substrates are not fluorescent per se. Only upon hydrolysis, occurring within the cell, the C12 alone emits green fluorescence.

Consistently, wild type mouse embryonic fibroblasts (MEFs) incubated with either C12-Di-β-D-Glucoronide, C12-Di-β-D-Glucopyranoside or C12-Di-β-D-Galactopyranoside at a concentration of 250µM exhibited a clear green fluorescent

labelling (due to substrate internalization from the medium, hydrolysis and release of the fluorescent product that remained intracellular-bound) mostly related to intracellular membranes (resembling lysosomal-like structures) (Figure 5).

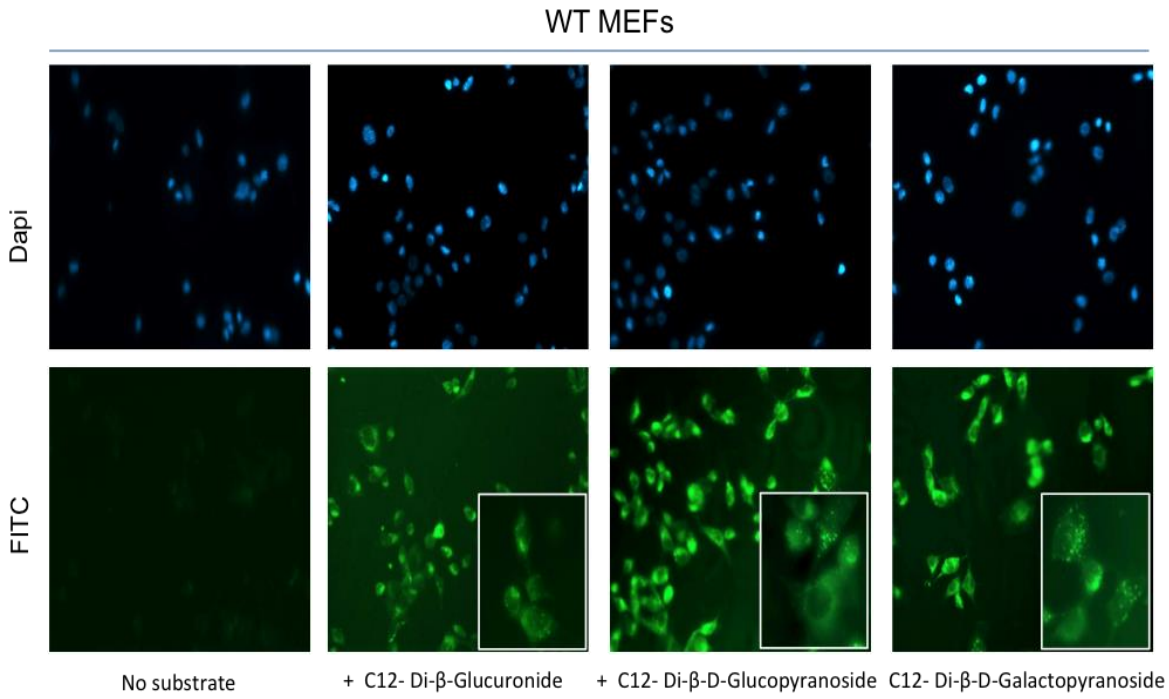

Figure 5. C12 fluorescent labelling of lysosomal enzymes activity in living MEFs evaluated at fluorescence microscope for GUSB, GBA and GLB1. Wild type MEFs were either incubated with C12-Di-β-D-Glucuronide, C12-Di-β-D-Glucopyranoside or C12-Di-β-D-Galactopyranoside at a concentration of 250µM for 1h or left untreated. Green fluorescence emission was then examined under FITC filter. Enlarged images showed that such fluorescence is mostly confined to intracellular membranes.

To demonstrate that C12 derived substrates 1) only emitted fluorescence upon hydrolysis by lysosomal enzymes within the cell, 2) once processed are unable to exit from the cells and 3) outside the cells, before the processing, are not fluorescence the conditioned medium of WT MEFs shown in figure 5 was analyzed for green fluorescence as well. No significant increase in the fluorescence was detected in the conditioned medium derived from cells treated with the different substrates compared to that from untreated cells (Figure 6).

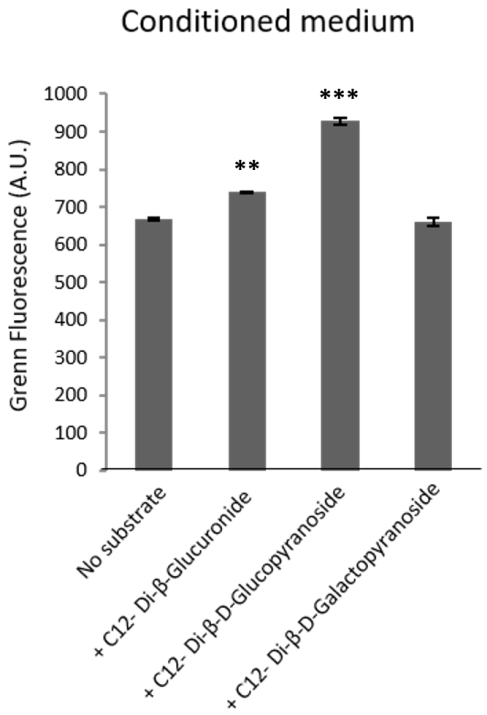

Figure 6. C12-derived substrates fluorescence analysis in conditioned medium from wild type MEFs. Green fluorescence emission in conditioned medium of wild-type MEFs either incubated with 250µM C12-Di-β-D-Glucuronide, C12-Di-β-D-Glucopyranoside or C12-Di-β-D-Galactopyranoside for 1h or left untreated. N=3, data represent the mean ± SEM. **p<0.005; ***p<0.0005.

The efficiency and sensitivity of intra-vital C12-derived fluorogenic substrates was then validated by fluorescence-activated cell sorting (FACS). The administration of substrates to wild-type fibroblasts induced a shift in green fluorescence of the cell population for all the three substrates analysed. Specifically, wild type and GUSB KO MEFs were treated with 250 µM C12-Di-β-D-Glucuronide and then detached and analysed at FACS for green fluorescence. WT cells exhibited a clear shift in green fluorescence, compared to untreated cells showing their capability to process the C12 derived substrate and above all the possibility to quantitatively evaluate GUSB enzymatic activity in living cells. Control GUSB KO cells did not exhibit any fluorescence upon substrate delivery (Figure 7).

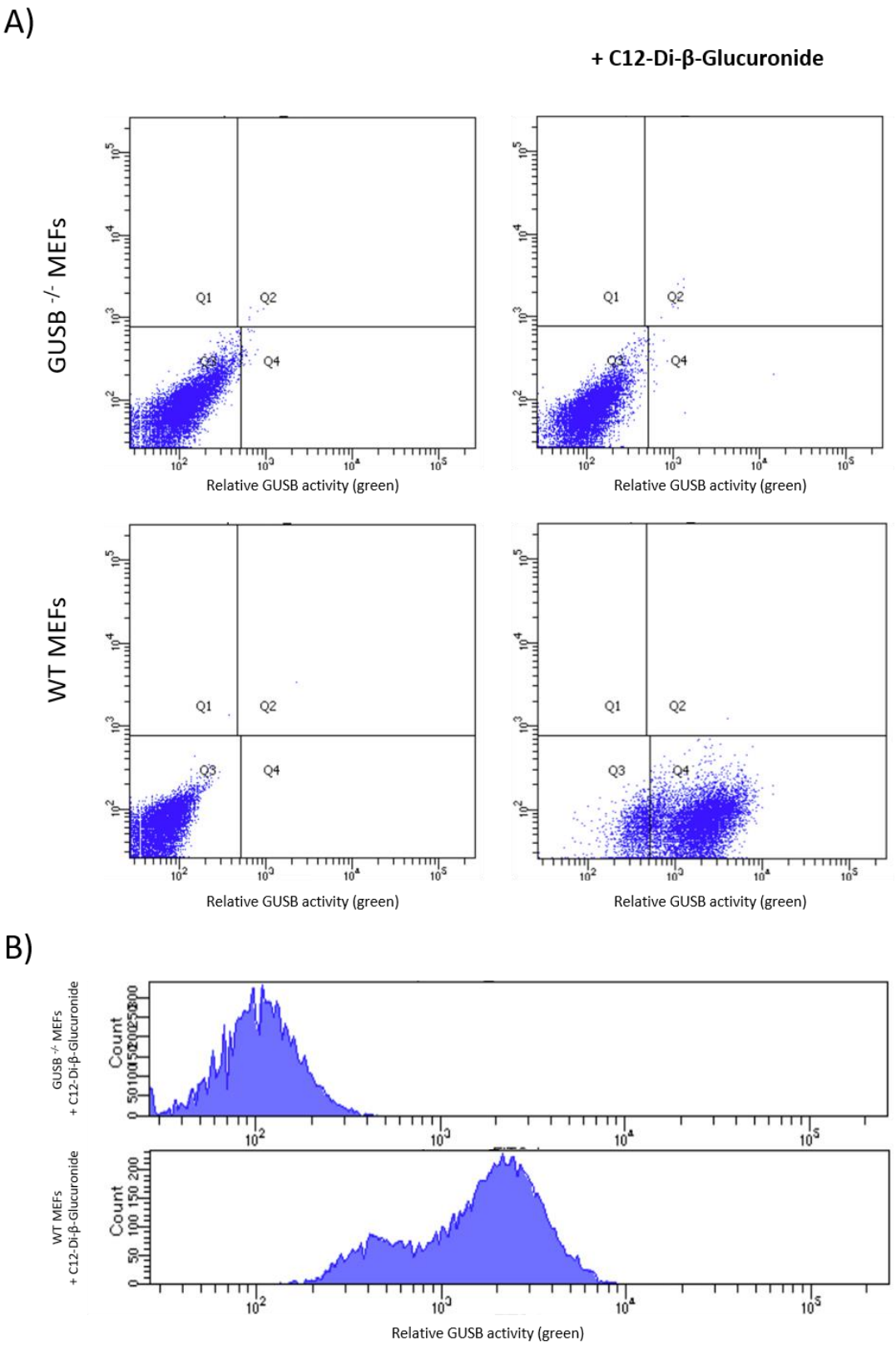

Figure 7. Enzymatic activity of GUSB enzyme measured by FACS in GUSB KO and WT MEFs. A) Representative FACS graph showing green fluorescence emission in GUSB-KO (upper panels) and WT (lower panels) MEFs either incubated with 250µM C12-Di-β-D-Glucoronide for 1h (right panels) or left untreated (left panels). B) Green fluorescent spectrum of treated GUSB-KO and WT MEFs. The y-axis represents the number of counted cells. Cells were synchronised with 2mM for 17h and detached with trypsin 0.05% EDTA. 10.000 cells were counted for each sample.

Similar results were obtained for GBA C12 derived substrate. Wild type and GBA KO MEF were treated with 250µM C12-Di-β-D-Glucopyranoside and then detached and analysed at FACS for green fluorescence. WT cells exhibited a sharp shift in green fluorescence showing their capability to process the C12 derived substrate and, also in this case, the possibility to quantitatively evaluate GBA enzymatic activity in living cells. Control GBA KO cells did not exhibit any fluorescence upon delivery of the fluorogenic substrate (Figure 8).

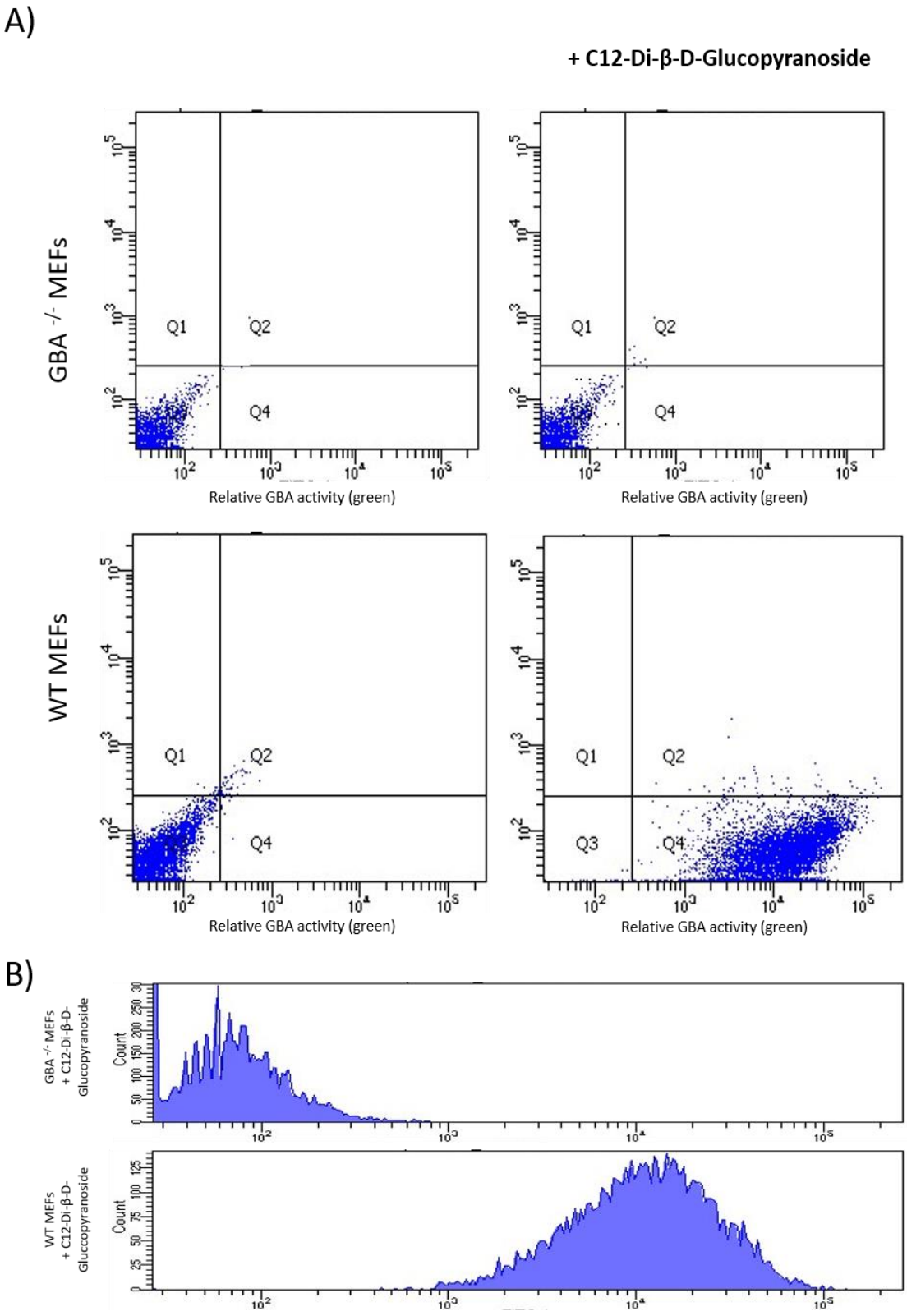

Figure 8. Enzymatic activity of GBA enzyme measured by FACS in GBA KO and WT MEFs. A) Representative FACS graph showing green fluorescence emission in GBA-KO (upper panels) and WT (lower panels) MEFs either incubated with 250µM C12-Di-β-D-Glucopyranoside for 1h (right panels) or left untreated (left panels). B) Green fluorescent spectrum of treated GBA-KO and WT MEFs. The y-axis represents the number of counted cells. Cells were synchronised with 2mM for 17h and detached with trypsin 0.05% EDTA. 10.000 cells were counted for each sample.

For the analysis of GLB1 activity human WT fibroblasts treated with 250µM C12-Di-β-D-Galactopyranoside were compared to fibroblasts derived from GM1 patients. In this case, the administration of the fluorogenic substrate induced a shift in green fluorescence in both cells lines due to a residual GLB1 enzymatic activity of GLB1 in GM1 cells. Interestingly, a relevant although moderate shift in green fluorescence is shown demonstrating the sensitivity of FACS analysis in discriminating the enzymatic activity (Figure 9).

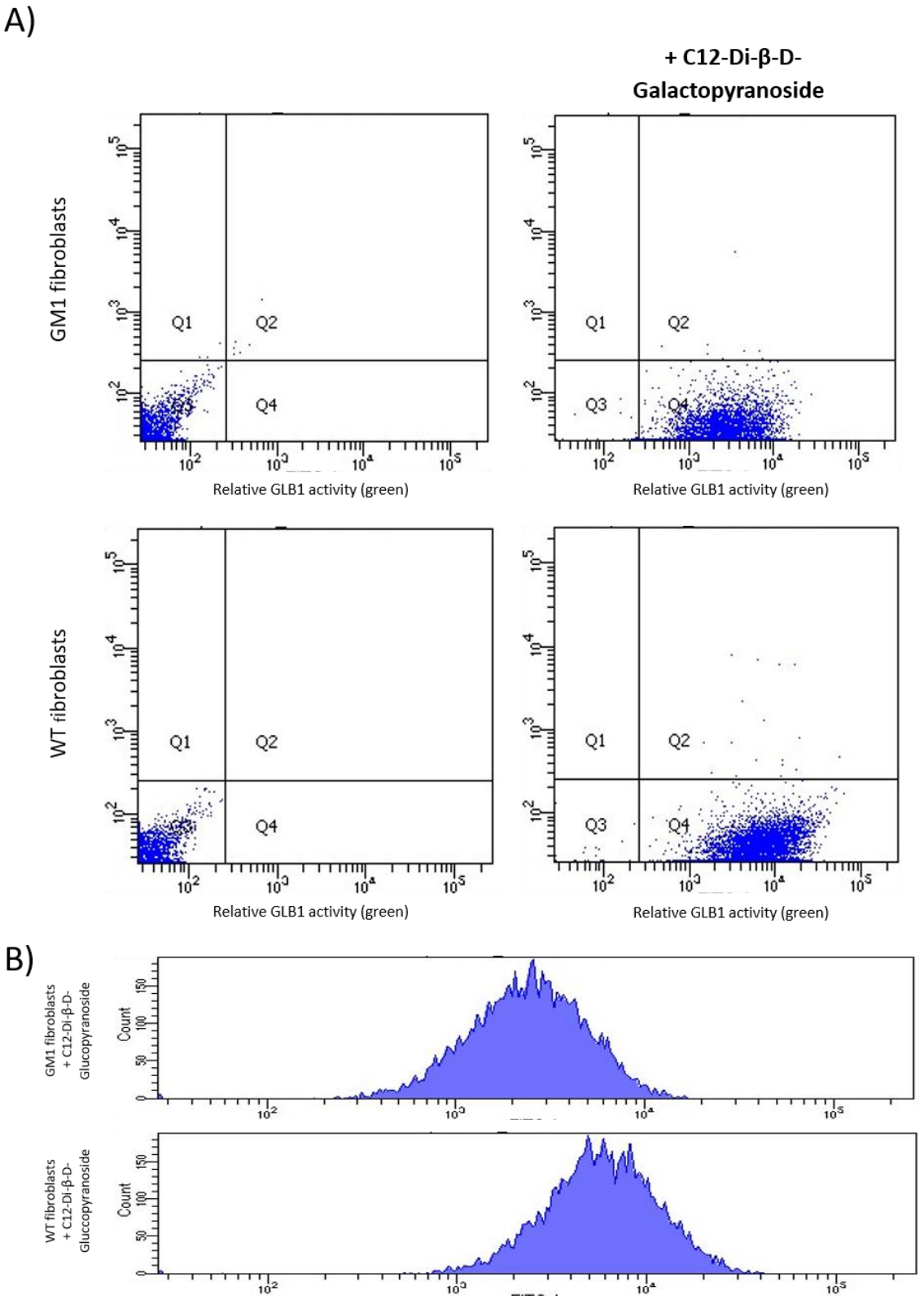

Figure 9. Enzymatic activity of β-gal enzyme measured by FACS in GM1 and WT human fibroblasts. A) Representative FACS graph showing green fluorescence emission in GM1 (upper panels) and WT (lower panels) human fibroblasts either incubated with 250μM C12-Di-β-D-Galactopyranoside for 1h (right panels) or left untreated (left panels). B) Green fluorescent spectrum of treated GM1 and WT human fibroblasts. The y-axis represents the number of counted cells. Cells were synchronised with 2mM for 17h and detached with trypsin 0.05% EDTA. 10.000 cells were counted for each sample.

These results not only confirmed what was evidenced from the previous experiment conducted on WT MEFs but also, and more importantly, demonstrated that is possible to evaluate by FASC the enzymatic activity of a specific lysosomal enzyme in living cells using C12 derived substrates.

7.3 A sensitive and quantitative FACS-based analysis for lysosomal hydrolases activity

In order to express the lysosomal enzymes and monitor their expression levels I used plasmids encoding for wild-type GBA, GUSB and β-galactosidase (β-gal) fused with a mCherry fluorescent tag bearing the 2A self-cleaving oligopeptide (enzyme-p2A-mCherry). The cDNA encoding each enzyme (GUSB, GBA1 or β-Gal) was cloned upstream the p2AmCherry cDNA sequence to generate plasmids expressing the respective fusion proteins (GUSBp2AmCherry, GBA1p2AmCherry and β-Galp2AmCherry). The mCherry fluorescent tag (red) allows the monitoring of the expression levels of lysosomal enzymes. All constructs also contained a flag tag at the C-terminal of each gene sequence (Figure 10).

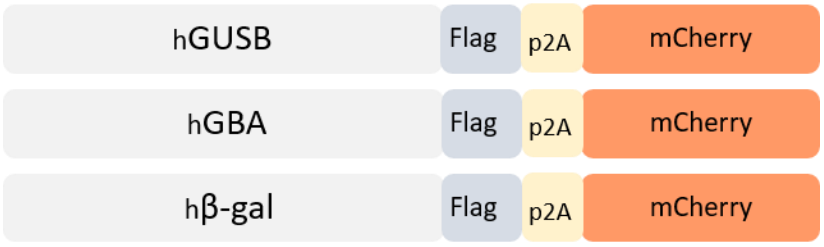

Figure 10. Schematic drowning of p2AmCherry constructs.

The 2A self-cleaving peptide is an oligopeptide (19–22 amino acids) that when located between two proteins undergo self-cleavage to generate two mature

proteins during translation (Ryan, King and Thomas, 1991) thus avoiding potential effect of the fluorescent tag on enzyme folding and activity (Figure 11).

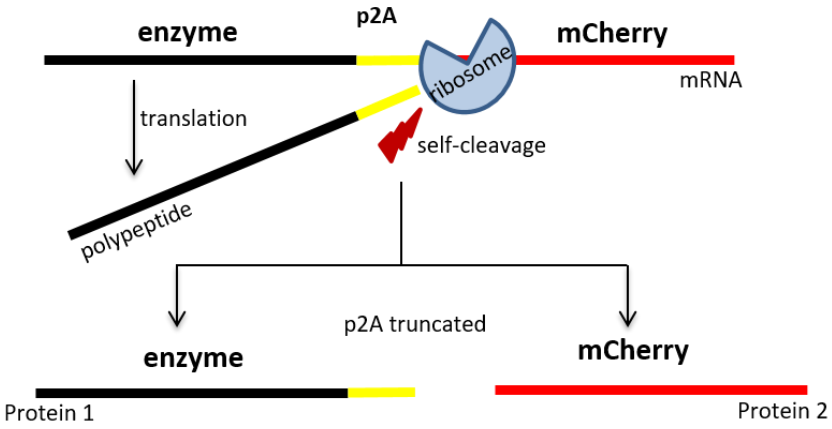

Figure 11. Schematic of p2A self-cleaving peptide functioning.

Anti-flag and anti-mCherry antibodies were used to evaluate the efficiency of the p2A self-cleaving system in wild-type MEFs transfected with the fusion proteins. Immunoblots showed efficient self-cleaving of all the three fusion proteins (Figure 12).

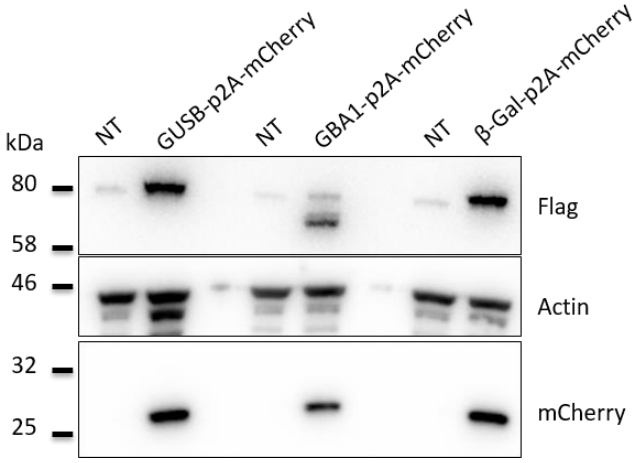

Figure 12. Expression of GUSB, GBA and β-gal with a self-cleaving mCherry tag. Western blot analysis using anti-flag and anti-mCherry antibodies showing efficient self-cleaving of mCherry peptide in MEFs transfected with the fusion proteins.

At this point, we were able to validate the FACS assay for GUSB. Cells were transfected with pGUSBp2Amcherry or pGBAp2Amcherry plasmids for 24h and then synchronised for 17h with thymidine a DNA synthesis inhibitor that can arrest cell at G1/S boundary, prior to DNA replication. After 24 hours the specific C12 substrate for each cell line was added to medium for 1 hour. Cells were then sorted in the flow cytometry for both red fluorescence (labelling the expression levels of the enzymes) and green fluorescence (labelling the enzymatic activity of lysosomal enzymes). FACS analysis showed that transfected cells exhibited an increase in the green fluorescence (as compared to control un-transfected cells) and the intensity of such green fluorescence well correlated with the amount of the mCherry expressed in analysed cells (red fluorescence) (Figure 13).

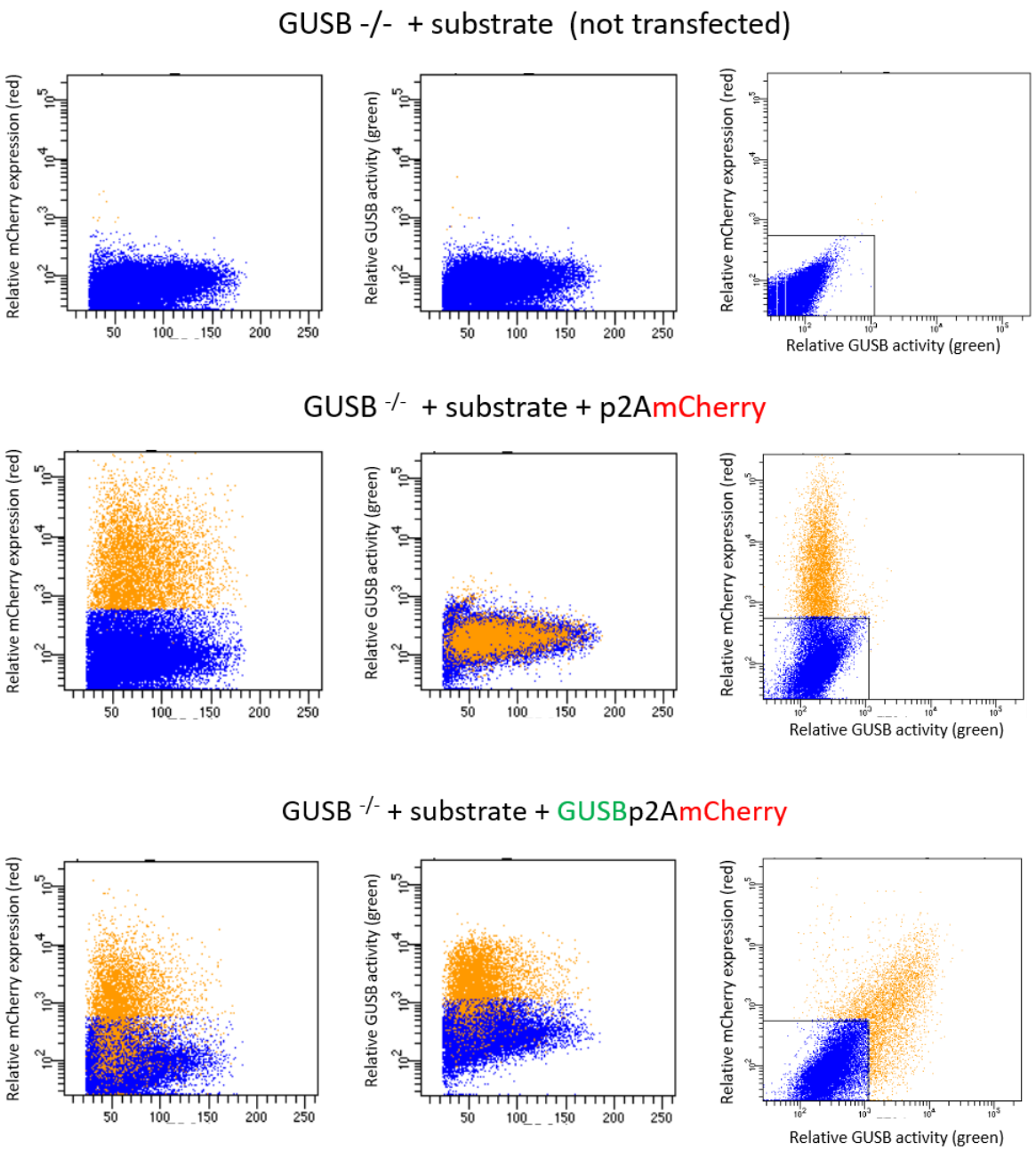

Figure 13. FACS assay validation for GUSB. Relative expression of mCherry (red fluorescence) and activity (green fluorescence) of GUSB measured by FACS in GUSB-KO MEFs transfected with either p2AmCherry or GUSBp2AmCherry plasmids or left untreated. Cells were synchronised with 2mM for 17h and then treated with 250µM C12-Di-β-D-Glucoronide for 1h or left untreated and subsequently detached with trypsin 0.05% EDTA. 10.000 cells were counted for each sample.

These data demonstrate that by using C12-derived fluorogenic substrates and the self-cleaving p2AmCherry tag the catalytic activity of exogenously expressed lysosomal enzymes can be labelled in intact cells analysed by FACS in a very sensitive and quantitative manner to identify and sort cells exhibiting enhanced enzymatic activity relatively to enzyme expression levels.

7.4 Validation of the FACS-based tool thought the analysis and discrimination of known GOF and LOF variants of GUSB

To demonstrate that this tool is able to discriminate between Loss-of-function and Gain-of-function mutants of a given enzyme I generated two known variants of GUSB showing altered enzymatic activity. Specifically, one known GUSB GOF variant showing a 8-10 fold higher enzymatic activity, when analyzed at pH 7.0, compared to the WT enzyme (E2-20 from Chen *et al.*, 2008) and one known GUSB LOF variant, responsible for a pathogenic condition, caused by a missense mutation (Lys606Asn), with a ~20% residual enzymatic activity (Tomatsu *et al.*, 2009). The mutated sequences were produced by direct mutagenesis and cloned into p2AmCherry vectors.

GUSB KO MEFs were transfected with plasmids encoding mCherry alone or mCherry fused with either GUSB*wt* (wild-type), GUSB*gain* (E2-20, gain-of-function mutant) or GUSB*loss* (Lys606Asn, loss-of-function mutant) and enzymatic activity assays were performed on lysates obtained from transfected MEFs. Specifically, the GOF mutant enzyme showed a tree-fold increase in enzymatic activity compared to WT enzyme, unlike what previously demonstrated by Chen *et al.* who described a 10 fold higher activity. However, it is important to underline that the activity of the E2-20 mutant has been originally evaluated at pH 7, while in this work lysosomal hydrolases activity is evaluated in physiological conditions for lysosomal enzymes functioning (pH ~5). This demonstrates that is possible to identify GOF mutants of lysosomal hydrolases at physiological conditions.

As expected, the LOF variant only showed 20% of residual activity compared to WT (Figure 14).

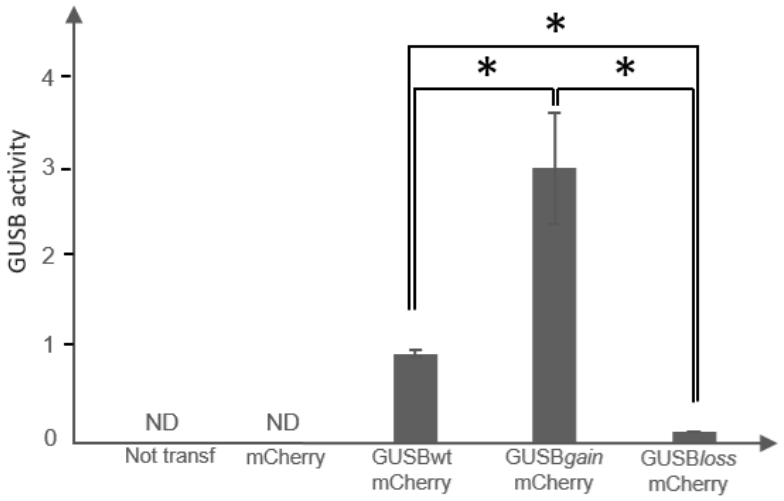

Figure 14. Enzymatic activity of GUSB variants in MEFs lysates. Graph is shown the enzymatic activity of GUSB enzyme variants along with controls measured at pH=5 in cells lysates derived from GUSB-KO MEFs transfected with plasmids encoding mCherry alone, GUSBwt-mCherry, GUSBgain-mCherry, GUSBloss-mCherry. Enzymatic activity was evaluated by 4-MU assay, normalized respect to both total protein amount and transfection efficiency and expressed as fold to WT. N=3, data represent the mean ± SEM. ND= not detected. *p<0.05.

This preliminary experiment demonstrated the functioning of both the GOF and LOF variants of GUSB that could then be employed to validate the FACS tool.

GUSB KO MEFs were then transfected again with plasmids encoding mCherry alone or mCherry fused with either GUSB*wt* (wild-type), GUSB*gain* (gain-of-function mutant), GUSB*loss* (loss-of-function mutant) and then synchronized and treated with C12-Di-β-D-Glucoronide. Cells were analyzed in the flow cytometry for both red and green fluorescence. The results showed that the population of cells transfected with mCherry plasmid (alone) (clearly distinguishable from control un-transfected cells since showed enhanced red fluorescence) did not exhibit any shift in green fluorescence (Figure 15 -blue). In contrast, the population of cells transfected with enzymep2AmCherry plasmids exhibited an increase in both the red and the green fluorescence (as compared to control cells) (Figure 15). Most importantly, the intensity of such green fluorescence correlated very well with the amount of the mCherry expressed in the analyzed cells (red fluorescence). To

further demonstrated the capability of FACS assays to quantitatively label enzymatic activities we used the known GUSB mutants previously employed in the enzymatic activity assay. KO MEFs were transfected with these mutants and analyzed by FACS upon C12 labeling. The results showed that the for the GOF mutant the distribution of transfected cells shifted toward higher values of green fluorescence, compared to cells transfected with WT enzyme, correlating with the increase in enzymatic activity showed in the enzymatic activity assay. While for LOF mutants, the cell distribution shifted towards lower values of enzymatic activity, compared to cells transfected with WT enzyme, and that such shift correlated with the residual activity of the transfected mutant (Figure 15).

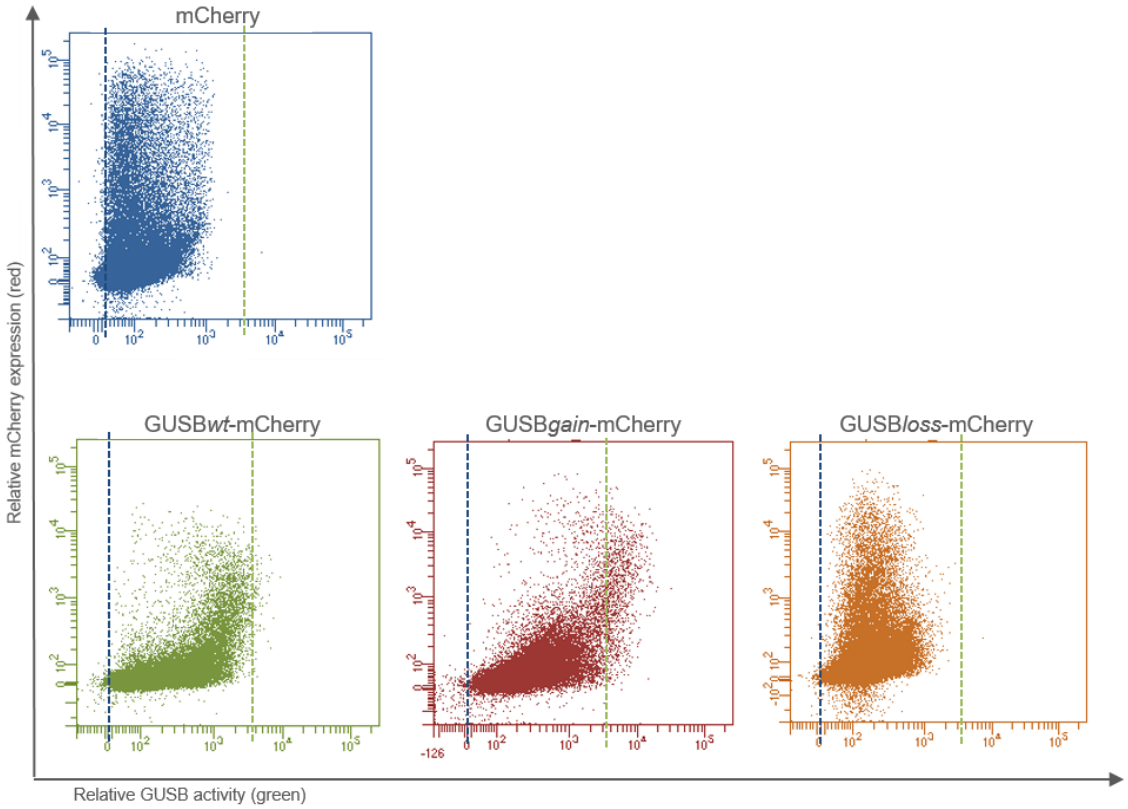

Figure 15. FACS analysis of GUSB known variants. Relative expression (red fluorescence) and activity (green fluorescence) of GUSB measured by FACS GUSB KO MEFs transfected with plasmids encoding mCherry alone (blue), GUSBwt-mCherry (green), GUSBgain-mCherry (red), GUSBloss-mCherry (orange). Cells were synchronised with 2mM for 17h and then treated with 250µM C12-Di-β-D-Glucoronide for 1h and subsequently detached with trypsin 0.05% EDTA. The entire amount of each sample was analysed.

Therefore, my results demonstrate that by using C-12-derived fluorogenic substrates and the self-cleaving p2AmCherry tag the catalytic activity of exogenously expressed lysosomal hydrolases can be labeled in FACS-analyzed intact cells in a very sensitive and quantitative manner. Cells exhibiting enhanced enzymatic activity relatively to enzyme expression levels can be sorted, thus supporting the suitability of such FACS-based tool for the identification of GOF variants of lysosomal enzymes. Importantly, such functional screening tool, for how it is conceived, could also pick up GOF variants with higher stability (longer half-life) rather than with higher catalytic performance since cells expressing enzyme with longer half-life may be able to process larger amount of substrate and thus exhibit increased green fluorescence relatively to the expression rate.

7.5 Identification of randomly generated activating mutations of GBA

Based on what demonstrated so far, using standard procedures based on error-prone PCR mutagenesis (McCullum *et al.*, 2010), I was able to generate a good quality randomly mutagenized p2Amcherry plasmid library for the cDNA encoding GBA with a diversity of ~2 x10^5 mutant variants and containing an average of 2/3 amino acid mutations per gene. The number of variants was estimated on the basis of the total number of bacterial colonies obtained from the plating of a fraction of competent cells transformed with the error-prone PCR products. The number of the obtained bacterial colonies was multiplied for the dilution factor of the total volume of the inoculum. Mutagenic conditions were specifically optimized for the GBA cDNA to obtain a number of mutations per sequence that was reasonably compatible with a gain-of-function (between 1-3 aminoacidic substitutions). The number of mutations was evaluated through Sanger sequencing analysis (Figure 16).

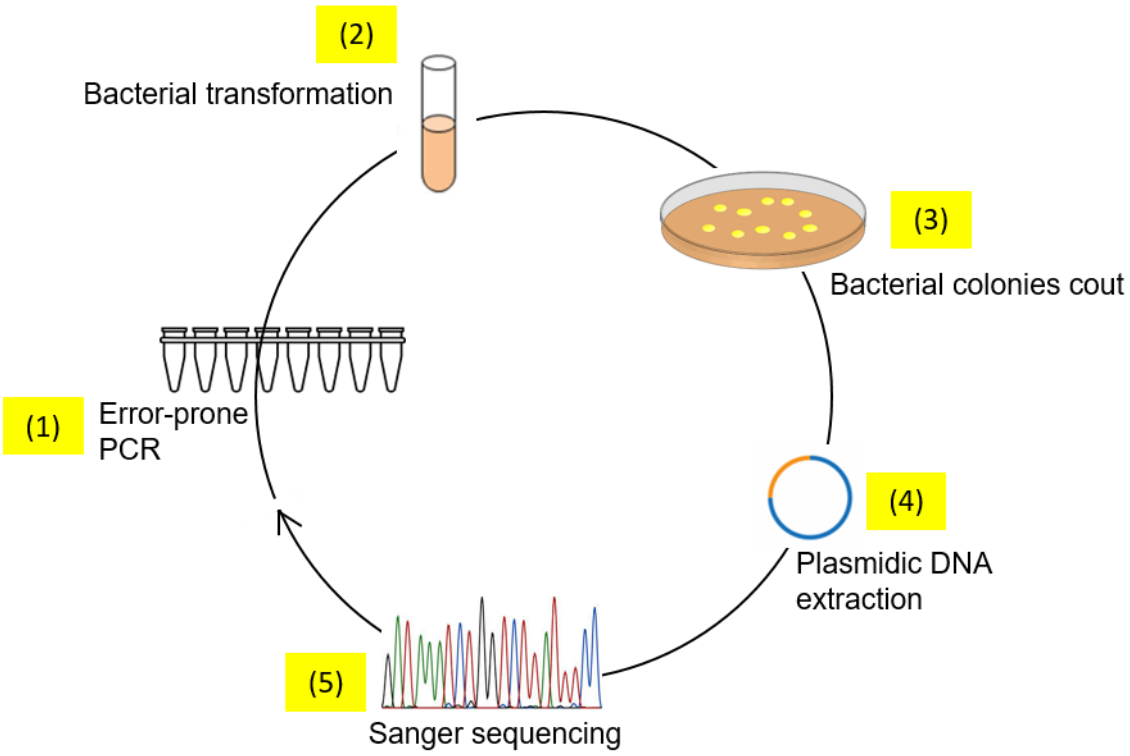

Figure 16. Random mutagenesis optimization for gain-of-function mutants. (1) Error-prone PCR to generate randomly mutagenized GBA plasmids (2) Transformation of mutagenized DNA into competent cells (3) Plating of aliquots of transformed competent cells and counting of obtained colonies (4) Plasmidic DNA extraction (5) Sequencing analysis of extracted DNA.

The GBA library has been then employed to produce a lentiviral library. In order to be packaged into lentiviral particles, the mutated constructs were cloned into the pLVX-EF1α-IRES-Puro vector, a bicistronic lentiviral expression vector that can be used to generate high-titer lentivirus. The vector contains an internal ribosomal entry site (IRES) that allows a gene-of-interest and a puromycin resistance gene.

The choice of a lentiviral library to vehicle the coding sequences into cells is based on the ability of lentiviruses to integrate their genome into that of the host cells ensuring a stable expression of the enzyme over time. Expression of the transcript is driven by the human elongation factor 1 alpha (EF1α) promoter, which continues to be constitutively active even after stable integration of the vector into the host cell genome. In order to maximize the probability that each cell would be infected

by one viral particle (so that cells would each express a single specific mutated enzyme variant) it was essential to employ a multiplicity of infection that allowed achieving a low infection rate (not higher than 20%) that was specifically calculated as 64 for the studied MEF cells. I performed the infection on GBA KO MEFs and 24h later, cells were exposed to puromycin in order to only select infected cells. At this point cells were sorted by FACS on the basis of both the red (mCherry) and green (C-12) fluorescence (Fig). Compared to cells infected with the WT GBA library cells infected with the randomly mutated GBA lentiviral library showed on the left part of the graph, a group of cells with low green fluorescence, likely expressing LOF variants of GBA. On the right part of the graph, cells infected with randomly mutated GBA lentiviral library showed a denser group of infected cells with an increased green fluorescence (~1,5% of the total cell population) that were isolated for further analisis. Among these, a large part showed higher GBA enzymatic activity (green) at relatively low level of mCherry expression (red) and, therefore, likely represented cells expressing GOF variants of GBA enzyme (Figure 17).

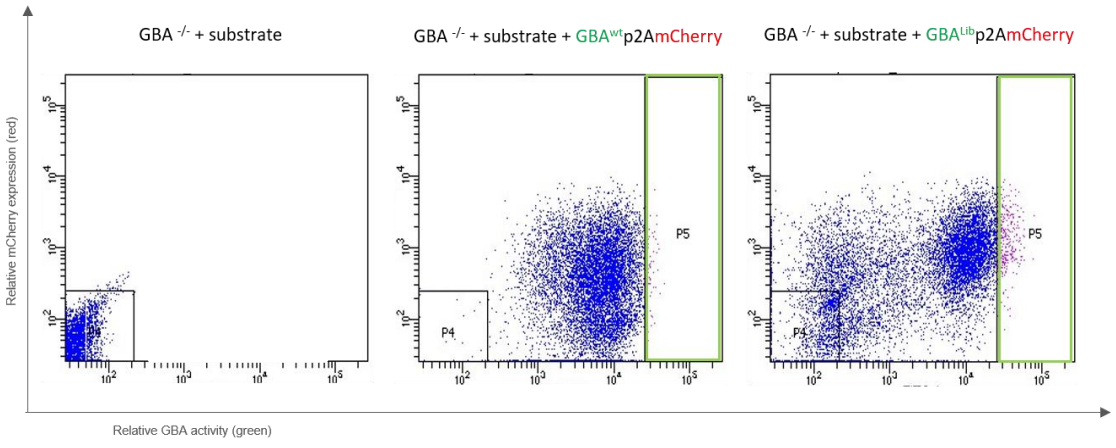

Figure 17. Representative experiment showing relative mCherry expression (red fluorescence) and activity (green fluorescence) of GBA measured by FACS in GBA-KO MEFs infected with lentiviral libraries either containing GBA^{wt}p2AmCherry or GBA^{mut}p2AmCherry plasmids or left untreated. Cells were infected with an MOI of 64 for 24 h and then selected in 3µg/ml puromycin for 72h. Cells were then treated with 250µM C12-Di-β-D-Glucopyranoside for 1h and detached with trypsin

0.05% EDTA. The entire amount of each sample was analysed. Green squares (P5) depict sorted cells. N=3.

Sorted cells were either cultured and expanded as a unique population or isolated to generate single clones in order to explore two different analysys strategies to identify possible gain-of-function mutants.

7.5.1 An unbiased approach for the identification of GBA activating mutations: deep sequencing analysis of enriched mutations

Genomic DNA was extracted from the cell fraction sorted form GBA KO MEFs infected with the mutated GBA library and sequenced by amplicon deep-sequencing (two separate biological replicates were produced). Sequencing reads were aligned to the reference GBA wild-type sequence in order to highlight the quality and location of the occurred mutations. The same procedure was performed on DNA extracted from an aliquot of the native lentiviral library employed for the infection. Finally, for each sample (including the viral library), the frequency of each found mutation (excluding silent mutations) was evaluated to address whether there was an enrichment of specific mutations within the studied population/virus. The results obtained from the cell samples were then compared to those obtained from the mutation analysis performed on the original viral library; interestingly the analysis shows that the enrichment in the two samples (S1 and S2) does not reflect the enrichment in the native viral library since those mutations found to be highly enriched in the native viral library resulted very poorly enriched in the sorted cell fractions and vice versa. Since the viral library contains the total number of randomly generated mutations where it is known that loss-of-function variants are statistically advantaged, it is possible to state that those mutations

found to be highly enriched in the viral library are indeed LOF variants that are poorly enriched in S1 and S2 as both generate from the fraction of infected cells exhibiting the highest GBA enzymatic activity. These results indicate that the enrichment is not a random event (Figure 18).

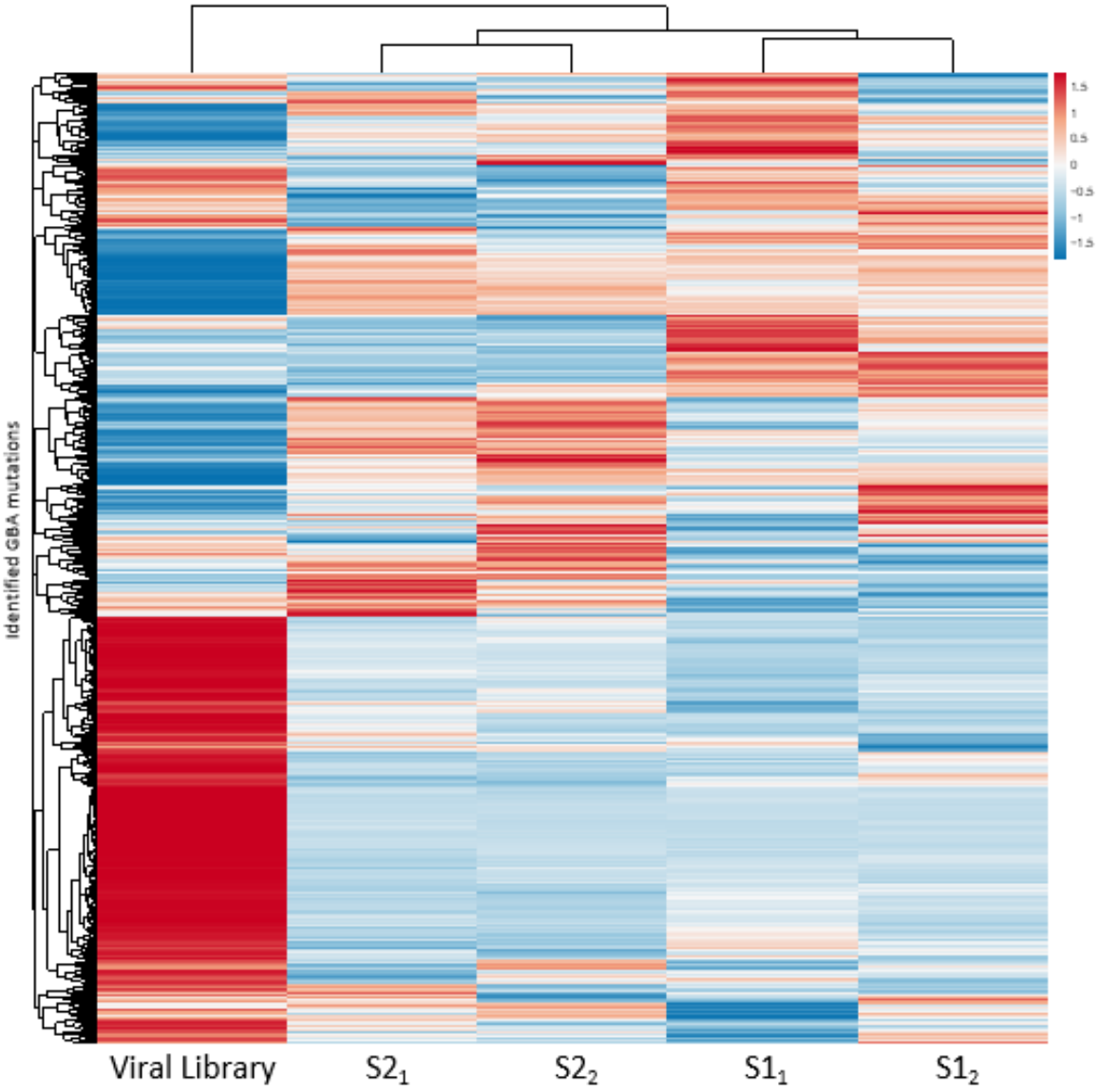

Figure 18. Heat Map of GBA mutations frequencies in sorted KO MEF cells. GBA mutations frequencies from most enriched (red) to less enriched (blue) normalized by the total number of input reads. Mutations in each sample (S1 and S2) were analysed in technical duplicate and compared to the mutations present in the native viral library. Hierarchical clustering based on Euclidean distance among samples (top) is shown.

For each sample, all the identified mutations were ranked on the basis of how much represented they were within the sample itself. Spearman Correlation was employed to perform a correlation analysis between samples. The Spearman's rank correlation is a measure between the rankings (i.e. relative position label of the observations within the variable: 1st, 2nd, 3rd, etc.) of two variables. The correlation between two variables will be high when observations have a similar rank between the two variables (correlation of 1 for an identical rank), and low when observations have a dissimilar rank between the two variables (correlation of −1 for a completely opposed rank).

The analysis showed a correlation between 83-95% demonstrating that samples shared very similar rankings (Figure 19).

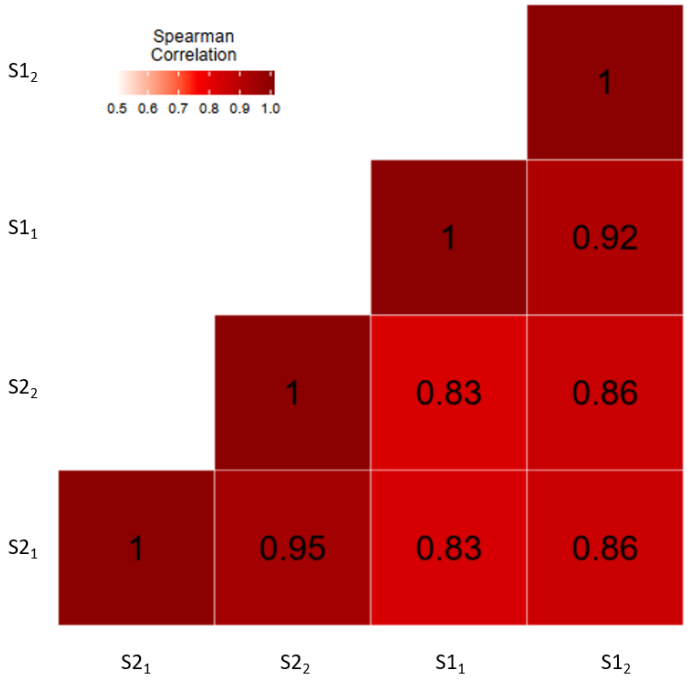

Figure 19. Correlation plot for GBA mutations libraries. Spearman correlation analysis between GBA libraries.

Finally, we looked at the overlap of the 32 most enriched mutations (99th percentile) of the libraries to individualise (if there were any) those shared between all the samples. We identified four mutations common to all the four libraries and three additional mutations common to three out of the four libraries analysed (Figure 20).

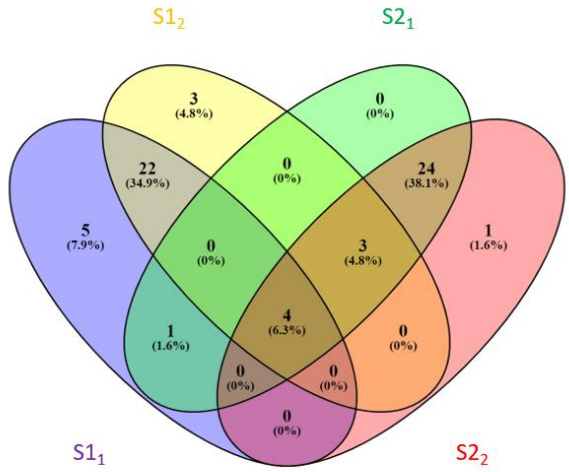

Figure 20. Identification of GBA most enriched mutations. VENN diagram showing the most enriched GBA mutations (32) identified in the sorted populations (each population is split into two technical duplicate).

Interestingly, the four mutations present in all the samples showed to be those with the highest score within each sample (Table 8).

POSITION	GBA REFERENCE NUCLEOTIDE	MUTATION	ENRICHEMENT SCORE S1$_1$	ENRICHEMENT SCORE S1$_2$	ENRICHEMENT SCORE S2$_1$	ENRICHEMENT SCORE S2$_2$
1341	G	C	115,20	82,36	144,61	297,63
1334	T	A	93,02	66,97	117,52	238,97
1340	A	C	39,70	28,47	49,28	100,43
1328	T	C	25,97	18,89	32,07	64,50
1238	A	T	-	11,52	164,48	163,12
1216	A	G	-	7,41	87,48	90,11
380	C	T	-	6,97	7,16	8,17

Table 8. TOP seven most enriched mutations of GBA library. Mutations (position and nucleotide substitution) are listed from most enriched (top) to less enriched (bottom). Enrichment scores of every mutation are reported for each sample.

7.5.2 A biased approach for the identification of GBA activating mutations: identification of cellular clones with increased enzymatic activity

Cells exhibiting high enzymatic activity at the FACS analysis, for both GBAmutp2AmCherry and GBAwtp2AmCherry (control) infected cell populations, were singularly sorted and cultured until they generated confluent clones that were collected and lysed. 4-MU assay was performed on cell lysates to evaluate GBA enzymatic activity. WT and KO MEFs were analysed as well as additional controls for the assay (Figure 21).

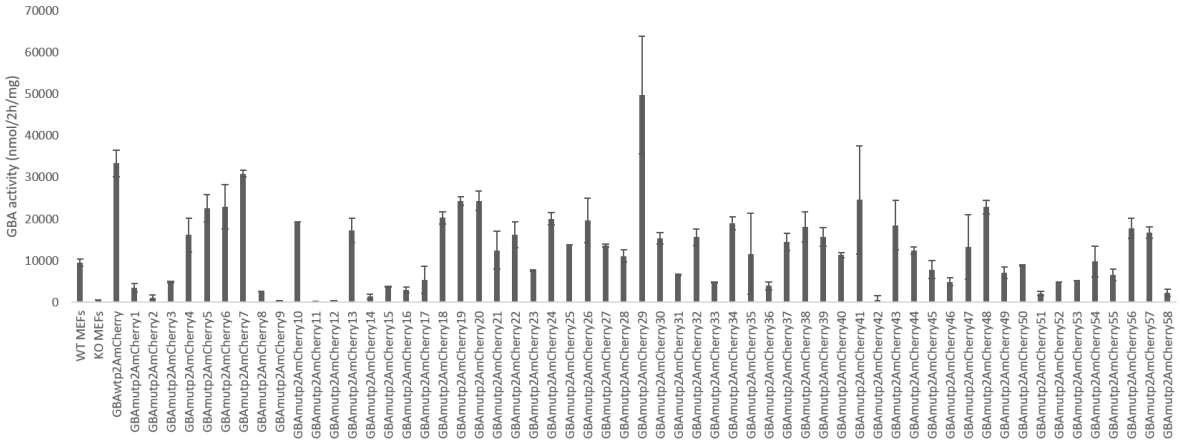

Figure 21. Enzymatic activity of GBA variants from lentiviral libraries infection in MEFs lysates. Graph is shown the enzymatic activity of GBA enzyme randomly mutated variants measured at pH=5 in cells lysates derived from GBA-KO MEFs transfected with plasmids encoding GBA^{wt}p2AmCherry or GBA^{mut}p2AmCherry or left untreated. WT MEFs represent a control for the assay. Enzymatic activity was evaluated by 4-MU assay, normalized respect to total protein amount, and expressed as nmol/2 hour/mg. N=2, Data represent the mean ± SEM. $p>0.05$.

Three clones, out of all those analyzed, were also subjected to sequence analysis (Sanger sequencing). Clones were chosen based on the results obtained from the enzymatic activity experiment and specifically: a WT-like clone (n.7, fig 21), a KO-like clone (n.42, fig 21) and the only clone showing increased GBA activity (n.29, fig 21) compared to controls. The sequences results showed between 2-4

mutations per sequence, as expected. Clone n7 showed two aminoacidic substitutions (Gly232Arg and Asn481Ser); clone n42 showed a nonsense mutation in position 293; clone n29 showed three missense mutations (Gly238Arg, Pro284Ala and Cys381Ser) and one silent mutation (Tyr259Tyr). Interestingly, the missense mutations identified in clone n29 were located in close proximity to GBA active sites: the proton donor Glu274 and the nucleophile Glu379, in the TIM barrel domain, a highly conserved domain among glycoside hydrolases and commonly involved in the enzymatic activity (Rigden, Jedrzejas and De Mello, 2003) (Figure 22).

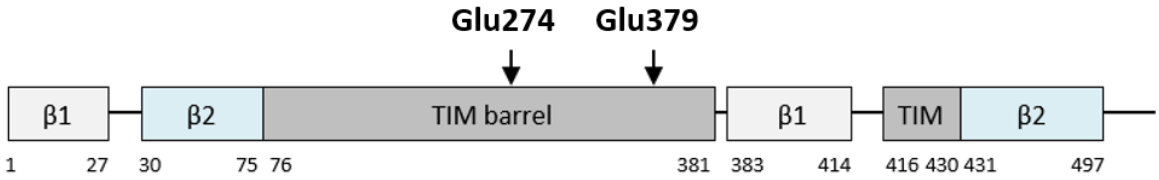

Figure 22. Schematic representations of mature form of hGBA. Domain organization of hGBA is shown: β1 domain (residues 1–27 and 383–414), β2 domain (residues 30–75 and 431–497) and TIM barrel domain (residues 76–381 and 416–430). Catalytic active sites are indicated with arrows.

We are now at the final validation step of the data obtained for GBA. The ten identified mutations have been already replicated in the GBA sequence through direct mutagenesis and will be tested soon, both singularly and in combinations. Their impact on GBA functionality will be evaluated *in vitro*, at a first instance. GBA variants activity will be evaluate on transfected cells and compared to the WT enzyme, and localization experiments will be performed as well to ensure that the modifications do not alter the trafficking pathways of the enzyme. If any of the tested mutation will exhibit clear increase in enzymatic activity with no other alteration in its functionality, then it will be re-evaluated, in an *in vivo* study to ensure that it is able to retain the increased activity *in vivo* and could represent a

valid alternative to set up a therapeutic strategy demonstrating the possibility to generate and identify lysosomal enzymes with improved therapeutic potential using our tool.

7.6 Alternative approaches to generate GOF variants of lysosomal hydrolases

In the attempt of generating hyperactive lysosomal hydrolase, I also decided to explore an alternative way. This strategy is not based on the generation of random mutations but rather on their customization. Specifically, it employs customised GBA mutants libraries designed based on GBA specific structure and function. Specifically, mutations are only located in the Tim barrel domain which is primarily involved in GBA functioning and represents a hotspot for GBA LOF mutations found in Gaucher disease patients (Figure 23).

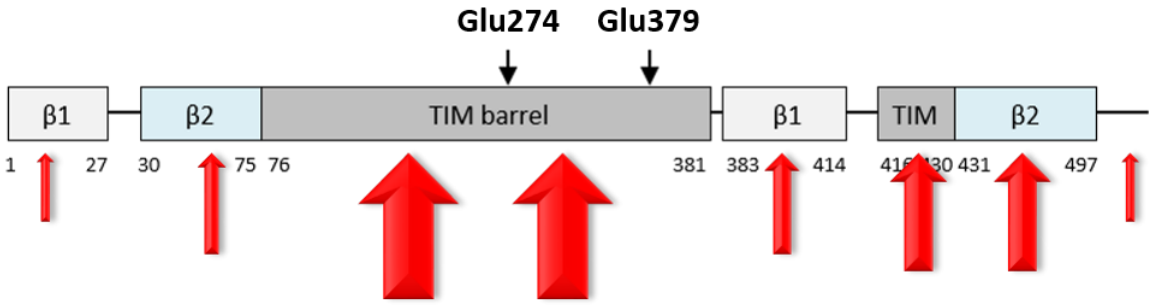

Figure 23. Schematic representation of GBA mutation hotspots. Red arrows indicate the regions mainly interested by mutations in patients affected by Gaucher disease**.** (bigger arrows indicate those regions interested by a wider range of mutations).

Given all this, the modification of this specific domain probably increases the chances to generate a GBA variant with altered enzymatic activity. Each sequence variant only has one aminoacidic substitution that replace each residue within the target sequence with all the remaining 19 amino acids. Customised libraries will be employed as already done with randomly mutagenized library. One advantage of customized libraries will be that the relatively low number of enzyme variants

generated by custom mutagenesis might allow the use of a bench-scale screening analysis based on enzymatic assays performed on individual clones generated by infected cells. Anyway, independently from the screening analysis used, the potential GOF mutations will be identified upon sequencing and then replicated in the GBA cDNA to be characterized as already described.

8. DISCUSSION

Although remarkable progresses have been made during the last two decades, with the development of innovative therapeutic strategies for lysosomal disorders, up to day, the treatment of LDSs remains very challenging. The primary purpose of treatments is to provide cells with the missing enzymatic activity responsible for the accumulation of material. The great majority of the established therapeutics strategy to treat LSDs is indeed aimed at increasing the missing enzyme function by either restoring its activity or replacing the dysfunctional enzyme (Parenti *et al.*, 2013). However, there is still great difficulty in achieving and maintaining therapeutic threshold levels of the corrective enzyme in targeted tissues, avoiding potential toxic effects caused by high dosage and/or repeated administration of therapeutic enzymes or vehicles. Thus, there is an urgent need to improve replacement therapy in lysosomal disorders for clinical purposes. The possibility of generating “ad hoc” gain-of-function versions of lysosomal enzymes may represent a powerful strategy to improve the available treatments of LSDs since these variants may produce a beneficial effect in targeted tissues at much lower doses and more efficiently compared to the respective WT enzymes.

I have developed a functional selection tool based on fluorescence-activated cell-sorting (FACS) that is capable to screen randomly generated mutated variants of lysosomal hydrolases and functionally select gain-of-function variants exhibiting enhanced catalytic activity and/or increased stability in physiological conditions. This functional selection tool employs optimized intra-vital fluorogenic substrates to specifically label in a very sensitive and quantitative manner the catalytic activity of lysosomal hydrolases in living cells and a mCherry fluorescent tag sequence to label the expression levels of the specific lysosomal hydrolase. Lentiviral-derived

libraries containing tagged mutated hydrolase variants are used to express the enzyme variants in cultured cells. Cells exhibiting enhanced enzymatic activity at are then sorted by FACS. These cells correspond to those expressing potential GOF variants. Coupling this tool with deep sequencing analysis and/or enzymatic activity analysis allows the identification of mutations present in such variants.

In the case of GBA I have already identified positive hits showing increased enzymatic activity (GOF mutations) by applying this functional selection tool to screen randomly mutagenized libraries. Specifically, seven mutations were identified by deep sequencing analysis while three mutations were identified through our biased approach based on enzymatic activity evaluation in expanded cell clones. Our data support the feasibility and suitability of the FACS-based tool I have developed to generate GOF variants of different lysosomal enzymes. These results clearly demonstrate the strength of our tool for the identification of randomly generated mutations in a given sequence, and thus its applicability to potentially every lysosomal enzyme. Of course, the possibility to apply our methods to other lysosomal enzymes depend on the availability of an appropriate C12-derived intravital fluorogenic substrate for the specific enzyme.

A very important analysis that represent the ongoing and the next future work is aimed at demonstrating that these variants identified by our methods properly localize to lysosomal compartment, can be secreted, thus cross-correcting other cells and are effective able to outperform *in vivo* over the WT counterpart. These studies will be important to move toward preclinical efficacy studies in animal models of disease.

9. REFERENCES

Adachi, M., Schneck, L. and Volk, B. W. (1974) 'Ultrastructural studies of eight cases of fetal Tay Sachs disease', *Laboratory Investigation*.

Andrews, S. (2010) 'FastQC', *Babraham Bioinformatics*. doi: citeulike-article-id:11583827.

Ballabio, A. *et al.* (2011) 'TFEB Links Autophagy to Lysosomal Biogenesis', *Science*.

Ballabio, A. and Gieselmann, V. (2009) 'Lysosomal disorders: From storage to cellular damage', *Biochimica et Biophysica Acta - Molecular Cell Research*. doi: 10.1016/j.bbamcr.2008.12.001.

Barton, N. W. *et al.* (1991) 'Replacement therapy for inherited enzyme deficiency — macrophage-targeted glucocerebrosidase for gaucher's disease', *New England Journal of Medicine*. doi: 10.1056/NEJM199105233242104.

Beck, M. (2018) 'Treatment strategies for lysosomal storage disorders', *Developmental Medicine and Child Neurology*, 60(1), pp. 13–18. doi: 10.1111/dmcn.13600.

Begley, D., Pontikis, C. and Scarpa, M. (2008) 'Lysosomal Storage Diseases and the Blood-Brain Barrier', *Current Pharmaceutical Design*. doi: 10.2174/138161208784705504.

Biffi, A. *et al.* (2004) 'Correction of metachromatic leukodystrophy in the mouse model by transplantation of genetically modified hematopoietic stem cells', *Journal of Clinical Investigation*. doi: 10.1172/JCI200419205.

Burré, J. *et al.* (2010) ‘α-Synuclein promotes SNARE-complex assembly in vivo and in vitro’, *Science*. doi: 10.1126/science.1195227.

Cang, C. *et al.* (2015) ‘TMEM175 Is an Organelle K+ Channel Regulating Lysosomal Function’, *Cell*. doi: 10.1016/j.cell.2015.08.002.

Cardone, M. *et al.* (2006) ‘Correction of Hunter syndrome in the MPSII mouse model by AAV2/8-mediated gene delivery’, *Human Molecular Genetics*. doi: 10.1093/hmg/ddl038.

Chen, K. C. *et al.* (2008) ‘Directed Evolution of a Lysosomal Enzyme with Enhanced Activity at Neutral pH by Mammalian Cell-Surface Display’, *Chemistry and Biology*. Elsevier Ltd, 15(12), pp. 1277–1286. doi: 10.1016/j.chembiol.2008.10.008.

Crudele, J. M. *et al.* (2015) ‘AAV liver expression of FIX-Padua prevents and eradicates FIX inhibitor without increasing thrombogenicity in hemophilia B dogs and mice’, *Blood*. doi: 10.1182/blood-2014-07-588194.

Cuervo, A. M. *et al.* (2004) ‘Impaired degradation of mutant α-synuclein by chaperone-mediated autophagy’, *Science*. doi: 10.1126/science.1101738.

Cuervo, A. M. and Dice, J. F. (2000) ‘When lysosomes get old’, *Experimental Gerontology*. doi: 10.1016/S0531-5565(00)00075-9.

Dittmer, F. *et al.* (1999) ‘Alternative mechanisms for trafficking of lysosomal enzymes in mannose 6-phosphate receptor-deficient mice are cell type-specific’, *Journal of Cell Science*.

Ellinwood, N. M. *et al.* (2011) ‘Safe, efficient, and reproducible gene therapy of the brain in the dog models of sanfilippo and hurler syndromes’, *Molecular Therapy*. doi: 10.1038/mt.2010.265.

Enquist, I. B. *et al.* (2007) ‘Murine models of acute neuronopathic Gaucher disease’, *Proceedings of the National Academy of Sciences of the United States of America*. doi: 10.1073/pnas.0708086104.

Eskelinen, E. L. (2006) ‘Roles of LAMP-1 and LAMP-2 in lysosome biogenesis and autophagy’, *Molecular Aspects of Medicine*. doi: 10.1016/j.mam.2006.08.005.

Eskelinen, E. L. and Saftig, P. (2009) ‘Autophagy: A lysosomal degradation pathway with a central role in health and disease’, *Biochimica et Biophysica Acta - Molecular Cell Research*. doi: 10.1016/j.bbamcr.2008.07.014.

Favret, J. M. *et al.* (2020) ‘Pre-clinical Mouse Models of Neurodegenerative Lysosomal Storage Diseases’, *Frontiers in Molecular Biosciences*. doi: 10.3389/fmolb.2020.00057.

Ferla, R. *et al.* (2013) ‘Gene therapy for mucopolysaccharidosis type VI Is effective in cats without pre-existing immunity to AAV8’, *Human Gene Therapy*. doi: 10.1089/hum.2012.179.

Ferreira, C. R. and Gahl, W. A. (2017) ‘Lysosomal storage diseases’, in *Metabolic Diseases: Foundations of Clinical Management, Genetics, and Pathology*. doi: 10.3233/978-1-61499-718-4-367.

Flanagan, J. J. *et al.* (2009) ‘The pharmacological chaperone 1-deoxynojirimycin increases the activity and lysosomal trafficking of multiple mutant forms of acid alpha-glucosidase’, *Human Mutation*. doi: 10.1002/humu.21121.

Fraldi, A. *et al.* (2010) ‘Lysosomal fusion and SNARE function are impaired by cholesterol accumulation in lysosomal storage disorders’, *EMBO Journal*. doi: 10.1038/emboj.2010.237.

Fraldi, A. *et al.* (2016) ‘Brain Disorders Due to Lysosomal Dysfunction’, *Annual*

Review of Neuroscience. doi: 10.1146/annurev-neuro-070815-014031.

Fraldi, A. *et al.* (2018) 'Gene therapy for mucopolysaccharidoses: in vivo and ex vivo approaches', *Italian Journal of Pediatrics*. doi: 10.1186/s13052-018-0565-y.

Freeman, D. *et al.* (2013) 'Alpha-Synuclein Induces Lysosomal Rupture and Cathepsin Dependent Reactive Oxygen Species Following Endocytosis', *PLoS ONE*. doi: 10.1371/journal.pone.0062143.

Fu, H. *et al.* (2010) 'Restoration of central nervous system α-N-acetylglucosaminidase activity and therapeutic benefits in mucopolysaccharidosis IIIB mice by a single intracisternal recombinant adeno-associated viral type 2 vector delivery', *Journal of Gene Medicine*. doi: 10.1002/jgm.1480.

Fuller, M., Meikle, P. J. and Hopwood, J. J. (2006) *Epidemiology of lysosomal storage diseases: an overview*, *Fabry Disease: Perspectives from 5 Years of FOS*.

Futerman, A. H. *et al.* (2004) 'New directions in the treatment of Gaucher disease', *Trends in Pharmacological Sciences*. doi: 10.1016/j.tips.2004.01.004.

Futerman, A. H. and Van Meer, G. (2004) 'The cell biology of lysosomal storage disorders', *Nature Reviews Molecular Cell Biology*. doi: 10.1038/nrm1423.

Gaudet, D. *et al.* (2013) 'Efficacy and long-term safety of alipogene tiparvovec (AAV1-LPL S447X) gene therapy for lipoprotein lipase deficiency: An open-label trial', *Gene Therapy*. doi: 10.1038/gt.2012.43.

Gentner, B. *et al.* (2010) 'Identification of hematopoietic stem cell-specific miRNAs enables gene therapy of globoid cell leukodystrophy', *Science Translational Medicine*. doi: 10.1126/scitranslmed.3001522.

Germain, D. P. and Fan, J. Q. (2009) 'Pharmacological chaperone therapy by

active-site-specific chaperones in Fabry disease: In vitro and preclinical studies', in *International Journal of Clinical Pharmacology and Therapeutics*.

Ghosh, P., Dahms, N. M. and Kornfeld, S. (2003) 'Mannose 6-phosphate receptors: New twists in the tale', *Nature Reviews Molecular Cell Biology*. doi: 10.1038/nrm1050.

Giugliani, R. *et al.* (2017) 'Intravenous infusion of iduronidase-IgG and its impact on the central nervous system in children with Hurler syndrome', *Molecular Genetics and Metabolism*. doi: 10.1016/j.ymgme.2016.11.121.

Goswami, R. *et al.* (2019a) 'Gene therapy leaves a vicious cycle', *Frontiers in Oncology*, 9(APR), pp. 1–25. doi: 10.3389/fonc.2019.00297.

Goswami, R. *et al.* (2019b) 'Gene therapy leaves a vicious cycle', *Frontiers in Oncology*. doi: 10.3389/fonc.2019.00297.

Graves, A. R. *et al.* (2008) 'The Cl-/H+ antiporter ClC-7 is the primary chloride permeation pathway in lysosomes', *Nature*. doi: 10.1038/nature06907.

Hamasaki, M. *et al.* (2013) 'Autophagosomes form at ER-mitochondria contact sites', *Nature*. doi: 10.1038/nature11910.

Haq, E. *et al.* (2006) 'Dysfunction of peroxisomes in twitcher mice brain: A possible mechanism of psychosine-induced disease', *Biochemical and Biophysical Research Communications*. doi: 10.1016/j.bbrc.2006.02.131.

Hara, T. *et al.* (2006) 'Suppression of basal autophagy in neural cells causes neurodegenerative disease in mice', *Nature*. doi: 10.1038/nature04724.

Harrison, F. *et al.* (2013) 'Hematopoietic stem cell gene therapy for the multisystemic lysosomal storage disorder cystinosis', *Molecular Therapy*. doi:

10.1038/mt.2012.214.

Haurigot, V. and Bosch, F. (2013) ‘Toward a gene therapy for neurological and somatic MPSIIIA’, *Rare Diseases*. doi: 10.4161/rdis.27209.

Ho, B. X. *et al.* (2018) ‘In vivo genome editing as a therapeutic approach’, *International Journal of Molecular Sciences*. doi: 10.3390/ijms19092721.

Hopwood, J. J. and Ballabio, A. (2001) ‘Multiple sulfatase deficiency and the nature of the sulfatase family’, *The Metabolic and Molecular Basis of Inherited Disease*.

Jeong, H. *et al.* (2009) ‘Acetylation Targets Mutant Huntingtin to Autophagosomes for Degradation’, *Cell*. doi: 10.1016/j.cell.2009.03.018.

Jessica L. Schneller *et al.* (2017) ‘Genome editing for inborn errors of metabolism: advancing towards the clinic’, *BMC Medicine*. doi: 10.1056/NEJMoa1300662.

Jones, S. A. *et al.* (2016) ‘A phase 1/2 study of intrathecal heparan-N-sulfatase in patients with mucopolysaccharidosis IIIA’, *Molecular Genetics and Metabolism*. doi: 10.1016/j.ymgme.2016.05.006.

Karolewski, B. A. and Wolfe, J. H. (2006) ‘Genetic correction of the fetal brain increases the lifespan of mice with the severe multisystemic disease mucopolysaccharidosis type VII’, *Molecular Therapy*. doi: 10.1016/j.ymthe.2006.02.012.

Kim, I., Rodriguez-Enriquez, S. and Lemasters, J. J. (2007) ‘Selective degradation of mitochondria by mitophagy’, *Archives of Biochemistry and Biophysics*. doi: 10.1016/j.abb.2007.03.034.

Kornfeld, S. and Sly, W. S. (2001) ‘I-Cell Disease and Pseudo-Hurler

Polydystrophy: Disorders of Lysosomal Enzyme Phosphorylation and Localization', *The Online Metabolic and Molecular Bases of Inherited Disease*.

Krueger, F. (2016) *Trim Galore*, *Babraham Bioinformatics*. doi: http://www.bioinformatics.babraham.ac.uk/projects/trim galore/.

Kurz, D. J. *et al.* (2000) 'Senescence-associated β-galactosidase reflects an increase in lysosomal mass during replicative ageing of human endothelial cells', *Journal of Cell Science*.

Langford-Smith, A. *et al.* (2012) 'Hematopoietic stem cell and gene therapy corrects primary neuropathology and behavior in mucopolysaccharidosis IIIA mice', *Molecular Therapy*. doi: 10.1038/mt.2012.82.

Langmead, B. and Salzberg, S. (2013) 'Bowtie2', *Nature methods*. doi: 10.1038/nmeth.1923.Fast.

Laplante, M. and Sabatini, D. M. (2012) 'MTOR signaling in growth control and disease', *Cell*. doi: 10.1016/j.cell.2012.03.017.

Lee, J. H. *et al.* (2010) 'Lysosomal proteolysis and autophagy require presenilin 1 and are disrupted by Alzheimer-related PS1 mutations', *Cell*. doi: 10.1016/j.cell.2010.05.008.

Lee, J. H. *et al.* (2015) 'Presenilin 1 Maintains Lysosomal Ca2+ Homeostasis via TRPML1 by Regulating vATPase-Mediated Lysosome Acidification', *Cell Reports*. doi: 10.1016/j.celrep.2015.07.050.

Li, H. *et al.* (2009) 'The Sequence Alignment/Map format and SAMtools', *Bioinformatics*. doi: 10.1093/bioinformatics/btp352.

Liang, S. Ben *et al.* (2007) 'Multiple reduced-intensity conditioning regimens

facilitate correction of fabry mice after transplantation of transduced cells', *Molecular Therapy*. doi: 10.1038/sj.mt.6300075.

Lieberman, A. P. *et al.* (2012) 'Autophagy in lysosomal storage disorders', *Autophagy*. doi: 10.4161/auto.19469.

Lindenbaum, P. (2015) 'JVarkit: java-based utilities for Bioinformatics', *Figshare*. doi: 10.6084/m9.figshare.1425030.v1.

Liu, L. *et al.* (2015) 'Glial lipid droplets and ROS induced by mitochondrial defects promote neurodegeneration', *Cell*. doi: 10.1016/j.cell.2014.12.019.

Macías-Vidal, J. *et al.* (2014) 'The proteasome inhibitor bortezomib reduced cholesterol accumulation in fibroblasts from Niemann-Pick type C patients carrying missense mutations', *FEBS Journal*. doi: 10.1111/febs.12954.

Di Malta, C. *et al.* (2012) 'Astrocyte dysfunction triggers neurodegeneration in a lysosomal storage disorder', *Proceedings of the National Academy of Sciences of the United States of America*. doi: 10.1073/pnas.1209577109.

Mancini, G. M. S., Havelaar, A. C. and Verheijen, F. W. (2000) 'Lysosomal transport disorders', in *Journal of Inherited Metabolic Disease*. doi: 10.1023/A:1005640214408.

Martina, J. A. *et al.* (2012) 'MTORC1 functions as a transcriptional regulator of autophagy by preventing nuclear transport of TFEB', *Autophagy*. doi: 10.4161/auto.19653.

Mazzulli, J. R. *et al.* (2011) 'Gaucher disease glucocerebrosidase and α-synuclein form a bidirectional pathogenic loop in synucleinopathies', *Cell*. doi: 10.1016/j.cell.2011.06.001.

McCullum, E. O. *et al.* (2010) ‘Random mutagenesis by error-prone PCR’, *Methods in Molecular Biology*. doi: 10.1007/978-1-60761-652-8_7.

Medina, D. L. *et al.* (2011) ‘Transcriptional activation of lysosomal exocytosis promotes cellular clearance’, *Developmental Cell*. doi: 10.1016/j.devcel.2011.07.016.

Medina, D. L. *et al.* (2015) ‘Lysosomal calcium signalling regulates autophagy through calcineurin and TFEB’, *Nature Cell Biology*. doi: 10.1038/ncb3114.

Mindell, J. A. (2012) ‘Lysosomal acidification mechanisms’, *Annual Review of Physiology*. doi: 10.1146/annurev-physiol-012110-142317.

Mizushima, N. (2007) ‘Autophagy: Process and function’, *Genes and Development*. doi: 10.1101/gad.1599207.

Monaco, A. *et al.* (2020) ‘The Amyloid Inhibitor CLR01 Relieves Autophagy and Ameliorates Neuropathology in a Severe Lysosomal Storage Disease’, *Molecular Therapy*. doi: 10.1016/j.ymthe.2020.02.005.

Motas, S. *et al.* (2016) ‘CNS-directed gene therapy for the treatment of neurologic and somatic mucopolysaccharidosis type II (Hunter syndrome)’, *JCI Insight*. doi: 10.1172/jci.insight.86696.

Mu, T. W. *et al.* (2008) ‘Chemical and Biological Approaches Synergize to Ameliorate Protein-Folding Diseases’, *Cell*. doi: 10.1016/j.cell.2008.06.037.

Napolitano, G. and Ballabio, A. (2016) ‘TFEB at a glance’, *Journal of Cell Science*, 129(13), pp. 2475–2481. doi: 10.1242/jcs.146365.

Nishino, I. *et al.* (2000) ‘Primary LAMP-2 deficiency causes X-linked vacoular cardiomyopathy and myopathy (Danon disease)’, *Nature*. doi: 10.1038/35022604.

Nixon, R. A., Yang, D. S. and Lee, J. H. (2008) 'Neurodegenerative lysosomal disorders: A continuum from development to late age', *Autophagy*. doi: 10.4161/auto.6259.

Orchard, P. J. *et al.* (2007) 'Hematopoietic Cell Therapy for Metabolic Disease', *Journal of Pediatrics*. doi: 10.1016/j.jpeds.2007.04.054.

Orchard, P. J. and Tolar, J. (2010) 'Transplant Outcomes in Leukodystrophies', *Seminars in Hematology*. doi: 10.1053/j.seminhematol.2009.10.006.

de Pablo-Latorre, R. *et al.* (2012) 'Impaired parkin-mediated mitochondrial targeting to autophagosomes differentially contributes to tissue pathology in lysosomal storage diseases', *Human Molecular Genetics*. doi: 10.1093/hmg/ddr610.

Palmieri, M. *et al.* (2011) 'Characterization of the CLEAR network reveals an integrated control of cellular clearance pathways', *Human Molecular Genetics*. doi: 10.1093/hmg/ddr306.

Parenti, G. *et al.* (2013) 'New strategies for the treatment of lysosomal storage diseases (Review)', *International Journal of Molecular Medicine*. doi: 10.3892/ijmm.2012.1187.

Parenti, G., Andria, G. and Valenzano, K. J. (2015) 'Pharmacological chaperone therapy: Preclinical development, clinical translation, and prospects for the treatment of lysosomal storage disorders', *Molecular Therapy*. doi: 10.1038/mt.2015.62.

Passarge, E. (2001) *Color Atlas of Genetics 2nd edition Passarge*, *Genetics*.

Patterson, M. C. *et al.* (2007) 'Miglustat for treatment of Niemann-Pick C disease: a randomised controlled study', *Lancet Neurology*. doi: 10.1016/S1474-

4422(07)70194-1.

Piccolo, P. and Brunetti-Pierri, N. (2015) ‘Gene therapy for inherited diseases of liver metabolism’, *Human Gene Therapy*, 26(4), pp. 186–192. doi: 10.1089/hum.2015.029.

Platt, F. M. *et al.* (1994) ‘N-butyldeoxynojirimycin is a novel inhibitor of glycolipid biosynthesis’, *Journal of Biological Chemistry*.

Platt, F. M., Boland, B. and van der Spoel, A. C. (2012) ‘Lysosomal storage disorders: The cellular impact of lysosomal dysfunction’, *Journal of Cell Biology*, 199(5), pp. 723–734. doi: 10.1083/jcb.201208152.

Platt, F. M. and Jeyakumar, M. (2008) ‘Substrate reduction therapy’, in *Acta Paediatrica, International Journal of Paediatrics*. doi: 10.1111/j.1651-2227.2008.00656.x.

Porto, C. *et al.* (2012) ‘Synergy between the pharmacological chaperone 1-deoxygalactonojirimycin and the human recombinant alpha-galactosidase A in cultured fibroblasts from patients with Fabry disease’, *Journal of Inherited Metabolic Disease*. doi: 10.1007/s10545-011-9424-3.

Prinetti, A. *et al.* (2011) ‘Secondary alterations of sphingolipid metabolism in lysosomal storage diseases’, *Neurochemical Research*. doi: 10.1007/s11064-010-0380-3.

Rajendran, L. and Annaert, W. (2012) ‘Membrane Trafficking Pathways in Alzheimer’s Disease’, *Traffic*. doi: 10.1111/j.1600-0854.2012.01332.x.

Rigden, D. J., Jedrzejas, M. J. and De Mello, L. V. (2003) ‘Identification and analysis of catalytic TIM barrel domains in seven further glycoside hydrolase families’, *FEBS Letters*. doi: 10.1016/S0014-5793(03)00481-2.

Roczniak-Ferguson, A. *et al.* (2012) ‘The transcription factor TFEB links mTORC1 signaling to transcriptional control of lysosome homeostasis’, *Science Signaling*. doi: 10.1126/scisignal.2002790.

Rogov, V. *et al.* (2014) ‘Interactions between Autophagy Receptors and Ubiquitin-like Proteins Form the Molecular Basis for Selective Autophagy’, *Molecular Cell*. doi: 10.1016/j.molcel.2013.12.014.

De Ru, M. H. *et al.* (2011) ‘Enzyme replacement therapy and/or hematopoietic stem cell transplantation at diagnosis in patients with mucopolysaccharidosis type I: Results of a European consensus procedure’, *Orphanet Journal of Rare Diseases*. doi: 10.1186/1750-1172-6-55.

Ryan, M. D., King, A. M. Q. and Thomas, G. P. (1991) ‘Cleavage of foot-and-mouth disease virus polyprotein is mediated by residues located within a 19 amino acid sequence’, *Journal of General Virology*. doi: 10.1099/0022-1317-72-11-2727.

S. Anson, D., McIntyre, C. and Byers, S. (2011) ‘Therapies for Neurological Disease in the Mucopolysaccharidoses’, *Current Gene Therapy*. doi: 10.2174/156652311794940791.

Sáez, P. J. *et al.* (2013) ‘Disruption in Connexin-Based Communication Is Associated with Intracellular Ca2+ Signal Alterations in Astrocytes from Niemann-Pick Type C Mice’, *PLoS ONE*. doi: 10.1371/journal.pone.0071361.

Saftig, P. and Klumperman, J. (2009) ‘Lysosome biogenesis and lysosomal membrane proteins: Trafficking meets function’, *Nature Reviews Molecular Cell Biology*. doi: 10.1038/nrm2745.

Sambri, I. *et al.* (2017) ‘Lysosomal dysfunction disrupts presynaptic maintenance and restoration of presynaptic function prevents neurodegeneration in lysosomal

storage diseases', *EMBO Molecular Medicine*. doi: 10.15252/emmm.201606965.

Sancak, Y. *et al.* (2010) 'Ragulator-rag complex targets mTORC1 to the lysosomal surface and is necessary for its activation by amino acids', *Cell*. doi: 10.1016/j.cell.2010.02.024.

Sardiello, M. *et al.* (2009) 'A gene network regulating lysosomal biogenesis and... [Science. 2009] - PubMed result', *Science (New York, N.Y.)*. doi: 10.1126/science.1174447.

Schaefer, K. A. *et al.* (2017) 'Unexpected mutations after CRISPR-Cas9 editing in vivo', *Nature Methods*. doi: 10.1038/nmeth.4293.

Settembre, C. *et al.* (2008) 'A block of autophagy in lysosomal storage disorders', *Human Molecular Genetics*. doi: 10.1093/hmg/ddm289.

Settembre, C. *et al.* (2013) 'Signals from the lysosome: A control centre for cellular clearance and energy metabolism', *Nature Reviews Molecular Cell Biology*. doi: 10.1038/nrm3565.

Shachar, T. *et al.* (2011) 'Lysosomal storage disorders and Parkinson's disease: Gaucher disease and beyond', *Movement Disorders*. doi: 10.1002/mds.23774.

Shen, D. *et al.* (2012) 'Lipid storage disorders block lysosomal trafficking by inhibiting a TRP channel and lysosomal calcium release', *Nature Communications*. doi: 10.1038/ncomms1735.

Singh, R. *et al.* (2009) 'Autophagy regulates lipid metabolism', *Nature*. doi: 10.1038/nature07976.

Sorrentino, N. C. *et al.* (2013) 'A highly secreted sulphamidase engineered to cross the blood-brain barrier corrects brain lesions of mice with

mucopolysaccharidoses type IIIA', *EMBO Molecular Medicine*. doi: 10.1002/emmm.201202083.

Spampanato, C. *et al.* (2011) 'Efficacy of a combined intracerebral and systemic gene delivery approach for the treatment of a severe lysosomal storage disorder', *Molecular Therapy*. doi: 10.1038/mt.2010.299.

Spillantini, M. G. *et al.* (1997) 'α-synuclein in Lewy bodies [8]', *Nature*. doi: 10.1038/42166.

Tardieu, M. *et al.* (2013) 'Intra cerebral administration of AAVrh.10 carrying human SGSH and SUMF1 cDNAs in children with MPSIIIA disease: Result of a phase I/II trial', *Human Gene Therapy*.

Tardieu, M. *et al.* (2017) 'Intracerebral administration of rAAV2/5hNAGLU vector in children with MPS IIIB: results at 30 months of a phase I/II trial', *Molecular Genetics and Metabolism*. doi: 10.1016/j.ymgme.2016.11.341.

Terman, A. *et al.* (2010) 'Mitochondrial Turnover and aging of long-lived postmitotic cells: The mitochondrial-lysosomal axis theory of aging', *Antioxidants and Redox Signaling*. doi: 10.1089/ars.2009.2598.

Tessitore, A. *et al.* (2004) 'GM1-ganglioside-mediated activation of the unfolded protein response causes neuronal death in a neurodegenerative gangliosidosis', *Molecular Cell*. doi: 10.1016/j.molcel.2004.08.029.

Van Til, N. P. *et al.* (2010) 'Lentiviral gene therapy of murine hematopoietic stem cells ameliorates the Pompe disease phenotype', *Blood*. doi: 10.1182/blood-2009-11-252874.

Tomatsu, S. *et al.* (2009) 'Mutations and polymorphisms in GUSB gene in mucopolysaccharidosis VII (sly syndrome)', *Human Mutation*. doi:

10.1002/humu.20828.

Vergarajauregui, S. and Puertollano, R. (2008) ‘Mucolipidosis type IV: The importance of functional lysosomes for efficient autophagy’, *Autophagy*. doi: 10.4161/auto.6567.

Visigalli, I. *et al.* (2010) ‘Gene therapy augments the efficacy of hematopoietic cell transplantation and fully corrects mucopolysaccharidosis type I phenotype in the mouse model’, *Blood*. doi: 10.1182/blood-2010-04-278234.

Vitner, E. B., Futerman, A. H. and Platt, N. (2015) ‘Innate immune responses in the brain of sphingolipid lysosomal storage diseases’, *Biological Chemistry*. doi: 10.1515/hsz-2014-0301.

Vitner, E. B., Platt, F. M. and Futerman, A. H. (2010) ‘Common and uncommon pathogenic cascades in lysosomal storage diseases’, *Journal of Biological Chemistry*. doi: 10.1074/jbc.R110.134452.

Vitry, S. *et al.* (2010) ‘Storage vesicles in neurons are related to Golgi complex alterations in mucopolysaccharidosis IIIB’, *American Journal of Pathology*. doi: 10.2353/ajpath.2010.100447.

Walker, F. O. (2007) ‘Huntington’s disease’, *Lancet*. doi: 10.1016/S0140-6736(07)60111-1.

Winslow, A. R. *et al.* (2010) ‘α-Synuclein impairs macroautophagy: Implications for Parkinson’s disease’, *Journal of Cell Biology*. doi: 10.1083/jcb.201003122.

Wolf, D. A. *et al.* (2011) ‘Direct gene transfer to the CNS prevents emergence of neurologic disease in a murine model of mucopolysaccharidosis type I’, *Neurobiology of Disease*. doi: 10.1016/j.nbd.2011.02.015.

Wu, Y. P. and Proia, R. L. (2004) ‘Deletion of macrophage-inflammatory protein 1α retards neurodegeneration in Sandhoff disease mice’, *Proceedings of the National Academy of Sciences of the United States of America*. doi: 10.1073/pnas.0400625101.

Yu, L. *et al.* (2010) ‘Termination of autophagy and reformation of lysosomes regulated by mTOR’, *Nature*. doi: 10.1038/nature09076.